A fully decentralized machine learning algorithm for optimal power flow with cooperative information exchange

Mohamed Lotfi [a,b], Gerardo J. Osório [c], Mohammad S. Javadi [b], Mohamed S. El Moursi [d], Cláudio Monteiro [a], João P.S. Catalão [a,b,*]

[a] Faculty of Engineering of the University of Porto (FEUP), R. Dr. Roberto Frias, 4200-465 Porto, Portugal
[b] INESC TEC, R. Dr. Roberto Frias, 4200-465 Porto, Portugal
[c] Portucalense University Infante D. Henrique (UPT), R. Dr. António Bernardino de Almeida, 4200-072 Porto Portugal
[d] Advanced Power and Energy Center, EECS Department, Khalifa University, Abu Dhabi, UAE

A B S T R A C T

Traditional power grids, being highly centralized in terms of generation, economy, and operation, continually employed probabilistic methods to account for load uncertainties. In modern smart grids (SG), rapid proliferation of non-dispatchable generation (physical decentralization) and liberal markets (market decentralization) leads to dismantling of the centralized paradigm, with operation being performed by several decentralized agents. Handling uncertainty in this new paradigm is aggravated due to 1) a vastly increased number of uncertainty sources, and 2) decentralized agents only having access to local data and limited information on other parts of the grid. A major problem identified in modern and future SGs is the need for fully decentralized optimal operation techniques that are computationally efficient, highly accurate, and do not jeopardize data privacy and security of individual agents. Machine learning (ML) techniques, being successors to traditional probabilistic methods are identified as a solution to this problem. In this paper, a conceptual model is constructed for the transition from a fully centralized operation of a SG to a decentralized one, proposing the transition scheme between the two paradigms. A novel ML algorithm for fully decentralized operation is proposed, formulated, implemented, and tested. The proposed algorithm relies solely on local historical data for local agents to accurately predict their optimal control actions without knowledge of the physical system model or access to historical data of other agents. The capability of cloud-based cooperative information exchange was augmented through a new concept of s-index activation codes, being encoded vectors shared between agents to improve their operation without sharing raw information. The algorithm is tested on a modified IEEE 24-bus test system and synthetically generating historical data based on typical load profiles. A week-ahead high-resolution (15-minute) fully decentralized operation case is tested. The algorithm is shown to guarantee less than 0.1% error compared to a centralized solution and to outperform a neural network (NN). The algorithm is exceptionally accurate while being highly computationally efficient and has great potential as a versatile model for fully decentralized operation of SGs.

1. Introduction

1.1. Background and motivation

Despite the profound differences between modern smart grids (SG) and traditional power systems, the primary function remains unchanged: Achieve a balance between power generation and demand at the minimal cost while ensuring system reliability and stability. Optimal power flow (OPF) management is at the heart of this, aiming at identifying optimal generation capacity of controllable/dispatchable generators in a power grid such that the total demand is met. OPF ensures that an electrical power grid is operating at a minimal total cost given the current demand profile and its technical and security constraints. OPF analysis is indispensable for power system operators, being continuously employed to ensure that the system is running at minimal or near-minimal operating costs [2].

In a traditional power system, the system operator is a single central entity with access to all measurable variables in the power grid. Accordingly, constructing a deterministic AC power flow model is

List of acronyms		NW-KDE	Nadarya Watson Kernel Density Estimation
		OPF	Optimal Power Flow
DR	Demand Response	P2P	Peer-to-Peer
DSM	Demand-Side Management	ERSE	Portuguese Energy Regulation Services Entity
DER	Distributed Energy Resources	pf	Power Factor
FFT	Fast Fourier Transform	PLF	Probabilistic Load Flow
IoE	Internet-of-Energy	P-OPF	Probabilistic Optimal Power Flow
IoT	Internet-of-Things	PPF	Probabilistic Optimal Power Flow
KDE	Kernel Density Estimation	PDF	Probability Distribution Function
ML	Machine Learning	RTS	Reliability Test System
MAPE	Mean Absolute Percentage Error	RES	Renewable Energy Resources
MC	Monte-Carlo	SG	Smart Grid

possible [19]. The AC-OPF thus incorporates all constraints, including the available generators' costs and limitations, grid structure, and associated safety constraints (e.g. bus voltage angle and transmission line power limits), to obtain the exact solution for ideal generation levels of individual generators. However, a deterministic AC power flow and the resulting AC-OPF models are both highly complex and highly non-linear, making it a formidable task to mathematically construct for each specific case, in addition to being computationally expensive to solve. Therefore, there has always been an interest in scientific literature to develop simplified and computationally efficient models, popularizing linear programming approaches [8,13].

Linearized OPF models do alleviate the mathematical complexity and computational expense. However, they suffer from critical drawbacks. First, the obtained solution, while deterministic in nature, is approximate and may lack in accuracy. Furthermore, linearization approaches can only be applied if the objective function(s) are differentiable and continuous, and they do not consider uncertain or unknown variables model [39].

The presence of the latter has been an issue even for traditional power systems. While a centralized system operator would have access to all measurable variables in the grid, uncertain parameters in the model persist for two reasons. First, in conventional power systems not all variables are constantly being metered or measured. Second, the increased presence of renewable energy sources (RES) as non-dispatchable sources inherently creates uncertain parameters in the model [12].

Alternatively, quasi-deterministic and probabilistic methods have been developed to solve for power flow and OPF in the presence of missing / unmeasurable data and RESs uncertainties [5]. Quasi-deterministic methods, such as Monte-Carlo (MC) simulations, account for uncertain variables by randomly generating a sufficiently large number of input samples to cover the entire uncertainty range and obtaining a deterministic solution for each sample. Thus, the uncertainty range of input variables is used to generate an uncertainty range of the outputs. While this provides accurate and complete information on grid behavior, it is often computationally expensive [5].

Probabilistic approaches employ statistical models to convert probability distributions of input parameters to those of the outputs. Those have a significantly higher computational efficiency and do not necessitate constructing a physical system model, however they require knowledge of the uncertain variables' probability distributions from a historical dataset, being predecessors to modern machine learning (ML) algorithms [3].

In order to clearly identify the state-of-the-art progress on the development of probabilistic and ML methods for new SG management paradigms which are discussed in Section 1.3, a literature review of the original probabilistic methods and their historical evolution is needed and is presented in Section 1.2.

1.2. Literature review: History of probabilistic methods for traditional power systems

Decades ago and prior to proliferation of renewable/non-dispatchable generation, stochastic behavior in power grids existed essentially on the load side; hence the original name: "Probabilistic Load Flow" (PLF) which is still used interchangeably with probabilistic power flow (PPF). [6] was one of the first papers to propose, implement, and test a PLF method for power system operation and planning.

The proposed method was used to obtain probability distribution functions (PDF) of branch (transmission line) power flows given those of input loads. First, three assumptions were made to simplify complex nonlinear equations: 1) linear relationship between branch flows and net nodal loads (linearized around expected values), 2) independence of active and reactive power, and 3) power balance is a function of the sum of input and output powers only (i.e. independent of individual nodal values).

Branch flow PDFs were then obtained by evaluating a recursive set of convolution integrations of the input and output PDFs. This could be used to obtain practically valuable information such as the probability of a line flow exceeding a certain value (e.g. capacity limit) or the realistically possible range for line loads. A major drawback of Borkowska's technique was that a very large number of convolution integrations that had to be evaluated. This restricted the method to smaller networks due to limitations of both computational speed and memory, especially at the time, limiting its applicability to real life scenarios.

In 1981, [4] realized this issue and exploited frequency domain multiplication with Fast Fourier Transforms (FFT) as a computationally efficient alternative to time domain convolution integration. The results proved FFT to be superior to convolution both in terms of computational efficiency and accuracy. In addition to proposing a more efficient PLF method, the study performed multiple important validation studies. First, the results of PLF were compared against those of MC-5000[1] for a case of high load value uncertainty (15x usual standard deviation). The results were highly similar with a slight skew in the PDFs which was not significant for practical applications where realistic uncertainties are much lower.

Second, the use of the central limit theorem was considered. Results showed that even when all inputs had a normal distribution, the output did not due to inherent system non-linearities. Therefore, it was concluded that the theorem should not be used regardless of system size. [4] later adapted the method to radial distribution networks, considering uncertainties in short-term (hourly) wind speed forecasts and corresponding uncertainties in produced active power and absorbed reactive power. [16] incorporated a probabilistic model for wind turbines to the original method.

---

[1] MC simulations are labeled as MC-X, where X is the total number of samples generated.

An alternative to convolution/FFT was proposed by [40]. The proposed algorithm relied on the statistical premise that two distributions with equal moments must also have equal cumulants. Thus, one can be computed from the other. The algorithm started by calculating moments, thereby the cumulants, of injected power. Linearized equations are then used to calculate cumulants, thereby the moments, of line flows. PDFs of line flows are finally constructed from their moments using Gram-Charlier expansion. The study found that at least 7th order Gram-Charlier expansions should be used to provide accurate output PDFs. The proposed approach was significantly faster than MC simulations.

The different variations of PLF mentioned so far are all characterized as analytical PLF methods (refer to Fig. 1). Analytical PLF methods still perform deterministic power flow calculations, however they employ statistical theories and probabilistic approaches to model the input uncertainties and determine the corresponding output uncertainty range in a computationally efficient manner (compared to quasi-deterministic methods).

Following the development of PLF techniques in literature, another category of PLF – approximate PLF – was being proposed. As will be shown subsequently, those are the direct predecessors of state-of-the-art work on probabilistic and ML algorithms of most recent literature. The main reason for the delay in developing approximate PLF techniques is that the statistical/mathematical theories they are based on were first discovered around the same time as PLF itself (the first point estimation method was published in 1975 [31], one year after Borkowski's paper). Moreover, more modern computing technologies motivated the application of such methods in the field of electrical power systems (the first point estimation method applied to PLF was in 2005, [34]).

While many point estimation methods were developed since then, they are all based on the same premise. Consider some variable y which is a function of random variables $\{v_1, v_2, \ldots v_{Nv}\}$. Let $y = f(v_1, v_2, \ldots v_{Nv})$ with f being a deterministic function and N_V being the number of random variables. A point estimation method is intended to approximate the first few moments of y and thereby estimate its PDF by evaluating f a number of times around each random input variable.

While this may seem similar to a MC simulation, the main and crucial difference lies in point estimation methods concentrating statistical information calculated on the points for each random input and thereby only requiring a significantly lower number of evaluations for a large number of random inputs. For comparison, MC has a complexity[2] of $O(M^N)$, varying exponentially with the grid size, or number of buses M, and the number of random variables N.

On the other hand, even the earliest point estimation methods are between $O(2N)$ and $O(4N)$ [26], varying linearly with larger problems, which is the same as analytical PLF methods, all while deterministic methods being more computationally efficient than convolutions, FFT, or cumulant-based evaluations. In addition, the linearization of the power flow equations ceases to be necessary, so in the case of high variance random variables in a network the original equations can be used, unlike analytical PLF.

[34] was the first to propose a PLF algorithm based on a point-estimation method in 2005. The method used is a "two-point" estimation one. I.e., two samples are evaluated for each random/uncertain variable, and therefore it is $O(2N)$, equivalent to Hong's point estimation [26]. The method was 25 times faster than MC with the results being in very good agreement. It should be noted that a relatively small network (6-bus) was used as the test case, so the implemented algorithm was assumed to run exponentially faster than MC for larger more complex networks.

This was verified a year later when [26] performed a more detailed

analysis using four different point estimation schemes, including the one proposed by [34]. A significantly larger network (118-bus) was used, and by comparing the resulting PDF's with MC simulations, it was concluded that $2N+1$ estimation schemes perform the best in terms of computational efficiency and provide high accuracy results even with a large number of random input (continuous or discrete) variables. The $2N+1$ point estimation was found to significantly outperform the $2N$ scheme used by [34] especially with a large number of random inputs, by performing only one additional calculation, and therefore it was recommended for use with large networks.

A simultaneous effort was underway to develop probabilistic models for the OPF and optimal dispatch problems. One of the pioneering papers to propose a probabilistic OPF (P-OPF) method was that of [36]. Dispatchable generators were modeled using second-order cost functions, and the control vector (for ideal generation levels) was modelled as a vector of PDFs by using Gram-Charlier expansion. The results showed excellent agreement with MC simulations for a small (8-bus) system, which was used as a test case due to limited computational capabilities of the time.

More than two decades later, [32] combined the work of [36 and 40] and proposed a cumulant-based P-OPF method. More modern computing technology allowed the method to be tested on a much larger 118-bus system. The simulations showed the proposed method provided highly accurate results with a computational efficiency an order of magnitude better than MC.

This section provided a review of some of the most influential papers in historic literature which pioneered the application of probabilistic and statistical theories to power flow and OPF methods (represented in Fig. 1). From this historical literature review, one can categorize power flow and OPF methods in traditional/centralized power systems into four categories (as shown in Fig. 2): deterministic, quasi-deterministic, analytical PPF, and approximate PPF. The different advantages and drawbacks of these methods are qualitatively compared in Table 1, according to the evaluated literature.

1.3. State-of-the-art review: Operation of modern smart grids

In modern SGs, Internet-of-Things (IoT) enabling creates an abundance of measured data from even the smallest devices in the system, which is in fact the main identifier of SGs compared to a traditional grid: implementation of smart metering and communication infrastructures [23,35].

This largely eliminates uncertainty caused by missing/unmeasurable variables in SGs. However, the combined effect of distributed energy resource (DER) proliferation, increased RESs penetration, and highly dynamic loads due to demand-side management (DSM) and demand response (DR) policies results in new sources of uncertainty, even for a centralized system operator with global data access [19,33].

On top of that, recent technological, societal, and policy changes are resulting in a call for decentralized operation of SGs, associated with paradigms whose names are increasingly seen in scientific and technical literature such as citizen-run energy communities, peer-to-peer (P2P) energy trading, and the Internet-of-Energy (IoE). In these paradigms, a transition from a centralized operation structure to a decentralized one is advocated [15].

While there are several technical, economical, and environmental benefits of this shift, it adds an additional layer of operational challenges. Contrary to a central operator, decentralized agents would only have access to local data, adding a significant level of uncertainty and inaccessible information from other parts of the grid. In this case, a deterministic power flow or OPF model is not possible to construct by multiple individual agents to whom information (including the physical model) on other regions of the grid may not always be known [29].

To deal with this challenge, two solution efforts exist. The deterministic approach involves the use of decomposition techniques, in which deterministic power flow or OPF global functions are decomposed
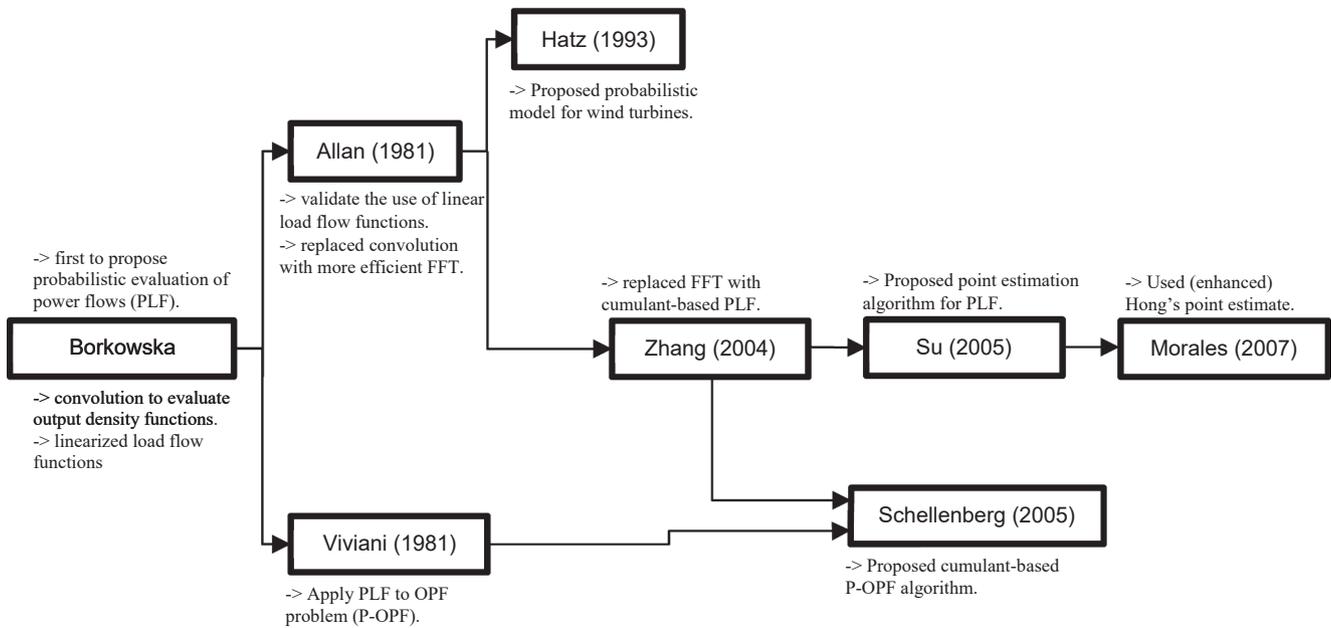
---

[2] MC simulations can be run with an infinitely large number of samples. The time complexity is based on the number of samples, more that which no numerically significant improvement is obtained (solution is converged).

Fig. 1. Historical timeline of pioneering papers in literature to apply statistical and probabilistic theories to power flow and OPF problems in traditional/centralized power systems.
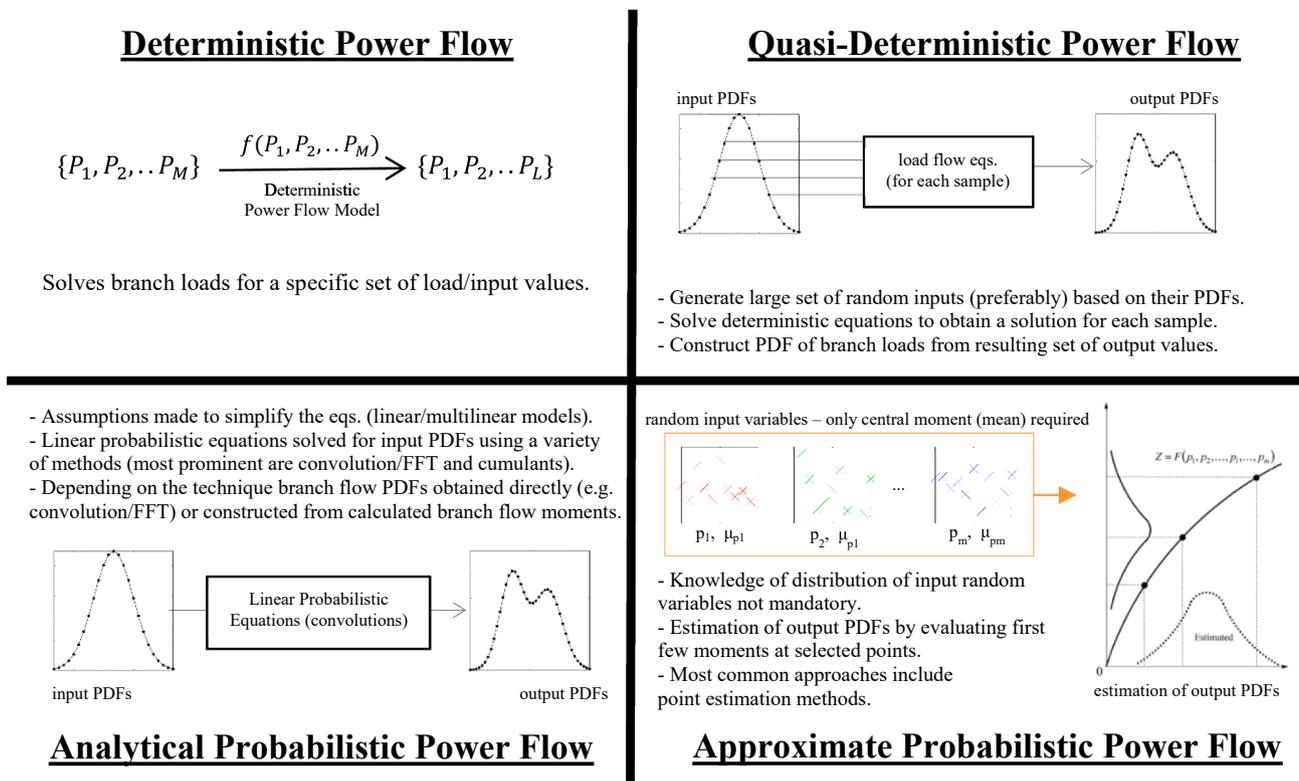

Fig. 2. Illustration and description of different categories of methods employed for power flow and OPF in traditional/centralized power systems.

into a set of local ones to be solved by individual agents, with each local function being dependent on the solutions of the local functions of other agents. Therefore, an iterative procedure is employed where local solutions are interchanged between agents until a convergence is achieved for all local functions i.e., global consensus found.

However, multiple drawbacks are associated with this approach. First, decomposition techniques often suffer from convergence issues and are difficult to generalize for use with a generic power system configuration (i.e., they must be tuned/configured for each system to achieve acceptable convergence). Second, the exchange of local function solutions between local agents must be highly synchronized for real-world applicability, making it heavily reliant on secure communication infrastructures with low latency. Finally, the incorporation of uncertain variables is very complex, if not impossible, in real-world applications [9,10,27].

This leads to the second solution effort, revisiting probabilistic

Table 1
Qualitative comparison of different categories of methods employed for power flow and OPF.

Category of PF/OPF Method	Deterministic	Quasi -Deterministic	Probabilistic (Analytical)	Probabilistic (Approximate)
Complexity of mathematical model / equations.	⊙⊙◎	⊙⊙◎	⊙⊙⊙	⊙◎◎
Complexity of computational implementation / program.	⊙⊙◎	⊙⊙◎	⊙⊙◎	⊙⊙⊙
Computational Expense (running time and memory)	⊙⊙◎	⊙⊙⊙	⊙⊙◎	⊙◎◎
Capability to incorporate uncertain / random variables.	×	✓	✓	✓
Grid physical model replaceable with historical data (ML extension possible).	×	×	×	✓

methods and their ML successors as viable solutions for the decentralized operation of SGs without the aforementioned problems. IoT-enabling and cloud computing capabilities now make it possible for probabilistic/ML algorithms to replace centralized system operators [3]. In traditional systems, the main drawback of these methods was reliance on historical data, which is no longer an issue in modern SGs (on the contrary, data redundancy is often brought up as an issue in the IoT paradigm).

The challenge in this case is to develop new algorithms in which agents can cooperate to achieve optimal global performance (as in OPF analysis), without sharing private/personal data to fit the new fully decentralized SG management paradigm [37]. Probabilistic and ML techniques make use of historical data to provide fast and accurate predictions of solution variables even in the presence of high levels of uncertainty. Moreover, these methods rely solely on statistical relationships between input and output variables without requiring a deterministic model of the physical system to be constructed [3,38].

This makes them ideal to deal with the aforementioned problems of decentralized operation. Moreover, they do not suffer the drawbacks of deterministic decomposition-based techniques (lack of general applicability, convergence issues, reliance on low-latency communication infrastructures, and difficulty to incorporate uncertain parameters) [20].

From the conducted review of pioneering works and the subsequent categorization of methods employed to traditional/centralized power systems, it was evident that the fourth category, approximate PPF/P-OPF methods are the predecessors of modern-day probabilistic and ML algorithms [3]. A major step in this evolution is the replacement of simple point estimates with non-parametric methods, which does not assume any statistical properties of the inputs to be known *a priori*.

Moreover, a point estimation (i.e., a deterministic calculation at the sampled points) is not needed and can be fully replaced with a historical dataset of input/output pairs, from which non-parametric methods directly estimate density distributions and corresponding output PDFs. Thus, the approach becomes purely a ML one where knowledge of a grid physical model is unnecessary. Kernel density estimation (KDE) has become the most popular non-parametric method in scientific literature, not only in the field of power systems but across the different applications of ML due to its reliability and computational efficiency [18].

[7] performed a two-stage P-OPF analysis on a grid with multiple wind farms. First, input PDFs of wind generation were estimated, followed by MC simulations in which sampling was done based on the generated PDFs. By constructing a combined PDF for all wind farms with wind speed dependence, its effects were analyzed on the P-OPF results as compared to using individual PDFs of the wind farms. By comparing KDE (non-parametric) and parameter estimation, the PDF produced by KDE and corresponding P-OPF results was found to be more accurate than parameter estimation.

Other studies such as [30] and [11] have performed similar analyses, in which KDE was used to estimate the PDFs of uncertain input variables (particularly from renewable generation).

The results of these studies are all in agreement with [7], verifying that the use of non-parametric methods in general and KDE in particular to estimate uncertain input variables in PPF is superior to parametric

techniques. The aforementioned studies solely employed KDE as a preprocessing method, performing quasi-deterministic power flow analysis rather than exploiting KDE's full potential to replace MC simulations for PPF, which was performed by other works in literature.

[21] applied KDE for PPF analysis of 14 and 118- bus systems with high levels of uncertainty and relying on historical operation data measurements. The method demonstrated accurate results with respect to the field measurements. In [28], a KDE-based method was proposed for PPF of unbalanced distribution networks. The method was tested on modified IEEE 13- and 37- bus test systems and compared against MC-3000 and $2 N + 1$ point estimation. The results showed that the proposed KDE-based PPF method was superior to both MC and point estimation both in terms of computational time and results accuracy.

[1] proposed and tested PPF algorithms based on holomorphic embedding, KDE, and saddle point approximation, comparing different approximate PPF techniques to analytical and quasi-deterministic ones. The proposed methods were tested on modified IEEE 14- and 118-bus test systems with high levels of uncertainty, and compared against MC-150000, $2 N + 1$ point estimation, and other methods.

The results clearly show the effectiveness of the proposed PPF methods and their superiority in terms of computational effort, while providing the same level of accuracy as MC simulations. The paper recognized the potential of approximate PPF methods in terms of their independence of the physical system model and flexibility in application, recommending their use for complex networks and energy management in modern SGs where historical operation data is available.

Aside from operation, the application of KDE-based methods is recently observed in other areas of SGs research, namely in forecasting. Indeed, by employing PPF/P-OPF based on historical data with a ML model, the problem is modeled similar to a forecasting problem in which a desired output is to be predicted based on historical inputs. Examples of this are [25] which proposed a cooperative forecasting model for electricity market prices based on KDE [22] which proposed a KDE-based ensemble algorithm for solar power forecasting.

1.4. Novel contributions and paper organization

In this work, a novel ML algorithm for fully decentralized power flow management of SGs is proposed, formulated, implemented, and tested. The proposed method was inspired by the forecasting models of [25] and [22], combining the cooperative approach of the former and the ensemble prediction of the latter. The novel contributions of this paper are listed as follows:

- A conceptual model is constructed for the transition from a fully centralized operation of a SG to a decentralized one, proposing the transition scheme between the two paradigms.
- In a fully decentralized SG run by local agents, a novel ML algorithm is proposed and formulated to enable this transition and into cloud-based fully decentralized system operation.
- The proposed algorithm relies solely on the local historical data for each agent to accurately predict optimal control action without being given any information on the physical system from outside their local zones (i.e., full grid structure is unknown), and without access to

historical data from other agents. As such, the proposed algorithm is designed not only to deal with variable uncertainties, but also missing / lacking information in a decentralized system.

• The proposed algorithm incorporates the capability of cloud-based cooperative information exchange without sharing private/raw data (e.g., local historical datasets or control actions taken locally). This is performed by proposing a new concept of an s-index vector, which is an encoded information that can be shared between agents to improve their control action predictions without sharing raw information.

The rest of this manuscript is organized as follows: In Section 2, the conceptual model of the proposed approach and its mathematical formulation are presented. In Section 3, the modified IEEE 24-bus test system which is used to test the proposed approach is detailed, along with the data used to generate the historical datasets. In Section 4, a high resolution (15-minute) week-ahead test case is performed for three different case studies, and the results are shown and validated against the deterministic solution based on AC-OPF. The studies investigate the effect of parameter tuning, impact of the incorporated cooperative information transaction model, and compare the performance with a Neural Network (NN). A discussion of the implications and limitations of the proposed algorithm is presented in Section 5, along with recommendations for future and follow-up work. The final conclusions are summarized in Section 6.

2. Proposed methodology

In this section, the conceptual model for decentralized operation of a SG is described. Then, the mathematical formulation of the proposed ML method for fully decentralized OPF management in this paradigm is presented. Finally, the cooperative information exchange capability of the proposed algorithm is illustrated.

2.1. Conceptual model

In Fig. 3, an illustration of the conceptual model for a transition between a centralized (left) and decentralized (right) operation paradigm for an electrical power grid is illustrated. In the centralized

paradigm, the system operator would have global access to all measurable variables in the system, and issue control signals to all controllable ones.

For a given grid, multiple overlaying models exist (e.g. corresponding to functions of real-time operation and dispatch, operation planning and unit commitment, voltage and frequency control, etc.). For each of those functions, the system operator would have a historical log of all input (measured) variables from the grid and the corresponding control actions taken (historical system states). In the case of OPF management, the logged historical system states can correspond to load values of the network and the corresponding ideal generation levels of all dispatchable generators.

On the right of Fig. 3, the decentralized paradigm is illustrated, in which the centralized system operator is replaced by individual agents. Agents control local regions, where the agent has direct access to measured variables and can issue control actions. The agents in this fully decentralized operation paradigm are speculated to be individual utility operators, small-scale energy communities, or autonomous microgrids as demonstrated by [24,27,35].

In the transition from the centralized to the decentralized paradigm, each agent would be handed over a subset of the system operator's historical dataset, only containing input/output variables specific to their respective zone. From this point onwards, agents utilize their individual historical datasets to manage local zones of control using a ML approach which continuously updates their datasets as new control signals are issued for new system states.

At the beginning of the transition the information inherited from the retired system operator, although partial, can guarantee accurate prediction of control actions which lead to both local and global optimization of system performance. However, with time the information provided from the time of the centralized paradigm becomes obsolete, and thus a continuous cooperation scheme between the agents is required to exchange useful information without having to share private and/or raw local data.

2.2. Generalized mathematical formulation

Consider a system that at any given instant has a set of measurable independent input variables **V**. To ensure global applicability of the
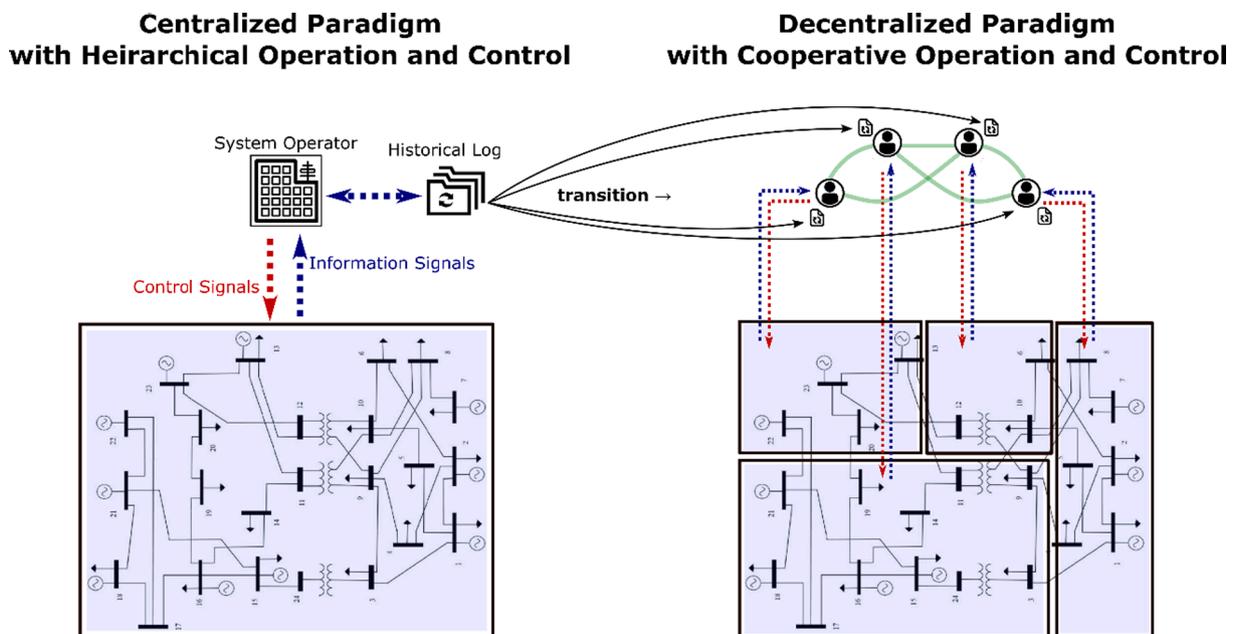

Fig. 3. An example illustration of the conceptual transition between a centralized (left) and decentralized (right) operation paradigm of power grids. Green lines correspond to information exchange.

developed ML method, all the system input variables are considered as uncertain variables (i.e., $|\mathbf{V}| = N_V$) as shown in (1). Moreover, no knowledge of the physical system model is known *a priori*, and thus no input variable interdependencies are assumed.

$$\mathbf{V} = \{v_1, v_2, \cdots, v_{N_V}\} \tag{1}$$

A set $\mathbf{Y}$ is defined in (2), containing N_y output variables, each of which is a function of the input vector, through an unknown system model, as shown in (3).

$$\mathbf{Y} = \{y_1, y_2, \cdots, y_{N_Y}\} \tag{2}$$

$$\mathbf{Y} = f(\mathbf{V}) = f(\{v_1, v_2, \cdots, v_{N_V}\}) \tag{3}$$

Thus for all recorded system states, a historical dataset of operation $\mathbf{H}$ exists for the system matching the input and output vectors as shown in (4)-(5).

$$\mathbf{H} = \{\boldsymbol{H}_1, \boldsymbol{H}_2, \cdots \boldsymbol{H}_{N_H}\} \tag{4}$$

$$H_k = \left\{ \underbrace{y_1^{hist,k}, y_2^{hist,k}, \cdots, y_{N_y}^{hist,k}}_{historical\ outputs\ at\ timestep\ k}, \underbrace{v_1^{hist,k}, v_2^{hist,k}, \cdots, v_{N_V}^{hist,k}}_{historical\ inputs\ at\ timestep\ k} \right\}, \quad \forall\, k = 1, 2, \cdots, N_H \tag{5}$$

For an updated system state, a new set of input variables $\mathbf{V}^{new}$ is measured as shown in (6), for which a corresponding set of output variables $\mathbf{Y}^{new}$ exists as shown in (7).

$$\mathbf{V}^{new} = \left\{ v_1^{new}, v_2^{new}, \cdots, v_{N_V}^{new} \right\} \tag{6}$$

$$\mathbf{Y}^{new} = f(\mathbf{V}^{new}) = f\left(\left\{ v_1^{new}, v_2^{new}, \cdots, v_{N_V}^{new} \right\} \right) \tag{7}$$

The objective of the proposed ML algorithm is to predict the value of Y^{new}, provided only V^{new} and $\mathbf{H}$, without any knowledge of the physical system model. The proposed ML algorithm (visualized in Fig. 4) is comprised of three main steps.

In the first step, a **similarity index (s-index)** between each historical system state and the new one is calculated using Nadarya-Watson KDE (NW-KDE), which evaluates a product of Gaussian kernel functions of all variables [25], as shown in (8), to obtain an s-index with a value between 0 and 1 for each historical state, resulting in the vector of s-indices $\mathbf{S}$ as shown in (9)-(10).

$$s_k = \left(\prod_i^{N_V} e^{-\frac{1}{2}\left(\frac{v_i^{hist,k} - v_i^{new}}{b_i}\right)^2} \right)^{\frac{1}{N_V}}, \quad \forall k = 1, 2, \cdots, N_H \tag{8}$$

$$0 \leq s_k \leq 1, \quad \forall k = 1, 2, \cdots, N_H \tag{9}$$

$$\mathbf{S} = \{s_1, s_2, \cdots s_{N_H}\} \tag{10}$$

For each variable i, the Gausian kernel function bandwidth b_i determines the sampling window relative to the statistical range of the historical samples of this variable. A coefficient α_i can be used to tune the individual bandwith value for each variable as shown in (9).

$$b_i = \alpha_i \left(\max_k\left(v_i^{hist,k}\right) - \min_k\left(v_i^{hist,k}\right) \right), \quad \forall k = 1, 2, \cdots, N_H, i = 1, 2, \cdots, N_V \tag{11}$$

Accordingly, α_i serves as a normalized tuning coefficient, whose value can be set between 0 (exclusive) and 1 (inclusive) as shown in (12), corresponding to a bandwidth value between zero (exclusive) and the maximum range of the historical values of the variable (inclusive).

$$0 < \alpha_i \leq 1, \quad \forall i = 1, 2, \cdots, N_V \tag{12}$$

The second step in the proposed method is to generate an activation vector for the most similar historical cases based on the calculated s-index vector. This can be done in two ways. First, a cut-off value can be set to activate all cases with an s-index above a certain value. The second, and the one used in this study, is to activate a fixed number of the
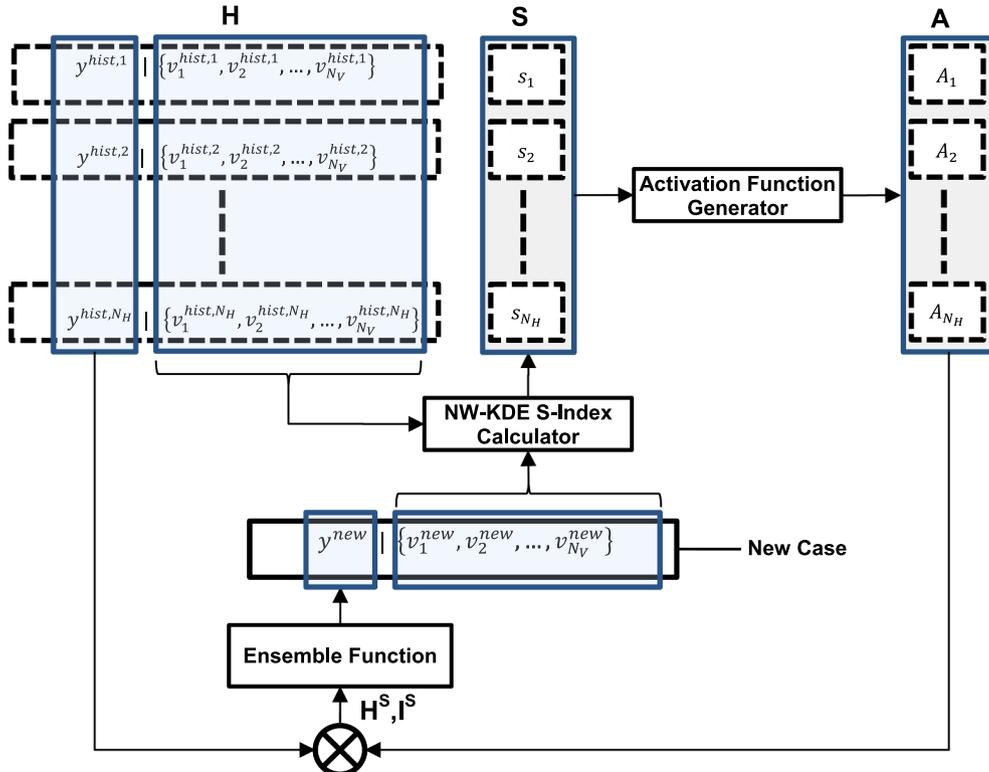

Fig. 4. Illustrative flowchart of the proposed and implemented ML algorithm.

top N_S historical cases from (highest N_S s-indices). In both cases, the result is an activation vector **A**, whose elements are binary values as shown in (13)-(14).

$$\mathbf{A} = \{A_1, A_2, \cdots, A_{N_H}\} \tag{13}$$

$$A_k \in \{0, 1\}, \quad \forall k = 1, 2, \cdots, N_H \tag{14}$$

The activation vector is used to extract the most similar cases from the historical dataset. Thus, a subset $\mathbf{H^S}$ is extracted by discarding all cases whose corresponding activation value is zero. The original indices of the extracted cases $\mathbf{H^S}$ (in the original set **H)** are preserved in vector $\mathbf{I^S}$. This is represented mathematically using (15)-(17) and is illustrated in Fig. 4.

$$H_k \in \mathbf{H^S} \Leftrightarrow A_k = 1 \forall k = 1, 2, \cdots, N_H \tag{15}$$

$$\mathbf{I^S} = \left\{ I_1^S, I_2^S, \cdots, I_{N_S}^S \right\} \tag{16}$$

$$\mathbf{H^S} = \left\{ H_{I_1^S}, H_{I_2^S}, \cdots H_{I_{N_S}^S} \right\} \tag{17}$$

The third and final step is to predict the output variables $\mathbf{Y^{new}}$ using an ensemble of the extracted most similar historical cases. The simplest approach is to calculate the mean value of each output variable from the extracted historical values as shown in (18).

Confidence intervals can be obtained by applying simple univariate KDE to obtain the out variables' PDFs and the corresponding confidence interval bounds as represented mathematically in (19)-(21), where $\rho_{1/2(x)\%}$ corresponds to the xth percentile. The lower and upper bounds of the xth percentile for each predicted output y_j^{new} are expressed as $\widehat{y}_{j,lb,x\%}^{new}$ and $\widehat{y}_{j,ub,x\%}^{new}$ as shown in (20) and (21), respectively.

$$y_j^{new} \approx \widehat{y}_j^{new} = \frac{\sum_{l=1}^{N_S} \left(y_j^{hist,I_l^S} \right)}{N_S}, \quad \forall j = 1, 2, \cdots, N_Y \tag{18}$$

$$\widehat{y}_{j,lb,x\%}^{new} \le \widehat{y}_j^{new} \le \widehat{y}_{j,ub,x\%}^{new}, \quad \forall j = 1, 2, \cdots, N_Y \tag{19}$$

$$\widehat{y}_{j,lb,x\%}^{new} = \rho_{\frac{1}{2}(100-x)\%} \left(\left\{ y_j^{hist,I_1^S}, y_j^{hist,I_2^S}, \cdots, y_j^{hist,I_{N_S}^S} \right\} \right), \quad \forall j = 1, 2, \cdots, N_Y \tag{20}$$

$$\widehat{y}_{j,ub,x\%}^{new} = \rho_{\frac{1}{2}(100+x)\%} \left(\left\{ y_j^{hist,I_1^S}, y_j^{hist,I_2^S}, \cdots, y_j^{hist,I_{N_S}^S} \right\} \right), \quad \forall j = 1, 2, \cdots, N_Y \tag{21}$$

2.3. Application to decentralized OPF with cooperative information exchange

In the case of an OPF problem, the input variables are the bus loads and the output variables are the ideal generation levels. In the decentralized operation paradigm, each agent would only have a historical dataset with variables in their regions of operation. From the presented mathematical formulation it can be seen that the proposed ML model is independent of the physical grid model, and thus even with a limited number of historical variables the prediction of the outputs can still be obtained.

One of the novel contributions of this paper is the capability of the proposed method to enable the cooperative information exchange without sharing private/raw data (e.g., local historical datasets or control actions taken locally). With the proposed method, this can effectively be performed by publicly sharing the activation vector **A** or the corresponding indices $\mathbf{I^S}$.

In this way, the exchanged indices of activated historical cases would greatly improve the output prediction of other agents by giving them

insight on relevant historical cases from the perspective of other agents and thereby the global performance of the system, without exposing any local/private information from the transacting agent's local database or the need for any central coordination. Accordingly, a distributed energy cloud operation scheme is enabled by the proposed method, as illustrated in Fig. 5.

The activation functions therefore serve as encoded, yet useful information which are broadcast into a public energy cloud shared accessible by all agents in the decentralized system. A few final remarks about the proposed algorithm and cooperation scheme are noted before proceeding to the case study and analysis:

- The size of the historical database does not need to be the same for all agents. In case a distributed energy cloud operation is adopted, standardized implementation is foreseen. However, even in the unlikely case where no standard database size is present activated historical cases can be shared based on their timestamps rather than index in the dataset.
- The tunable parameters of the proposed method are the normalized bandwidth coefficients α_i and NS. While tuning of these parameters can improve the prediction accuracy, it will be shown in the next sections that the proposed algorithm is highly versatile, such that applying default values for all the parameters still guarantees highly accurate output predictions.
- The proposed method is highly computationally efficient. While the computational implementation is demanding, all operations are based on simple direct array multiplications and manipulations. The high computational efficiency of the implementation will also be demonstrated in the next sections.
- The proposed algorithm was proposed and implemented as original code by the authors using MATLAB R2020b, on a standard laptop computer with an Intel Core i7-8550U CPU @ 1.80 GHz, 16.0 GB RAM, and a Windows 10 64-bit operating system.

3. Case study and validation analyses

3.1. Modified IEEE 24-bus test system

To demonstrate and validate the proposed algorithm, a case study was constructed based on a modified IEEE 24-bus reliability test system (RTS), whose single line diagram is shown in Fig. 6. The 24-bus network has 33 transmission lines, in addition to five transformers separating the two voltage levels in the network (138 kV and 230 kV). A total of 33 generators (G1, G2, … , G33), including one synchronous generator (G15), are incorporated.

For the purposes power flow analyses, active power generators that are both 1) connected to the same bus, and 2) have the same cost functions, are aggregated as a single generation station or utilities [14]. Applying this to the considered 24-bus RTS results in 14 utilities (U1, U2, … , U14) being the active power generation stations of the system. In the decentralized operation paradigm, these generation utilities are considered to be the decentralized operating agents of the system, spread across five zones of operation (Z1, Z2, Z3, Z4, Z5) as is also shown in Fig. 6.

The zones are listed in Table 2, including the corresponding buses and utilities therein. Accordingly, in the case of an OPF analysis, each utility as a decentralized operating agent has access only to historical load values from its own zone (i.e., loads at buses inside its zone).

The utilities do not have knowledge of each other's historical generation values (only their own). Table 3 lists all 14 utilities, the corresponding zone, incorporated generators, and their respective operating
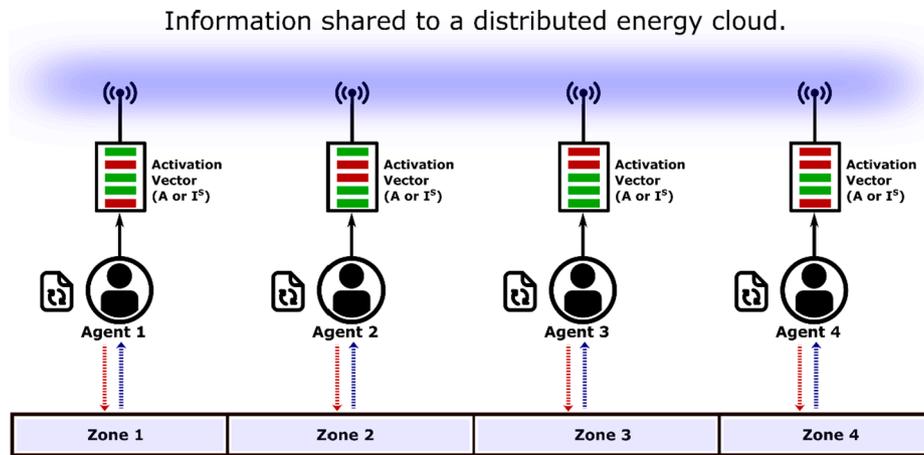
Information shared to a distributed energy cloud.

Fig. 5. Illustration of the cooperative information exchange made possible by the proposed and implemented ML algorithm, enabling a distributed energy cloud operation scheme.
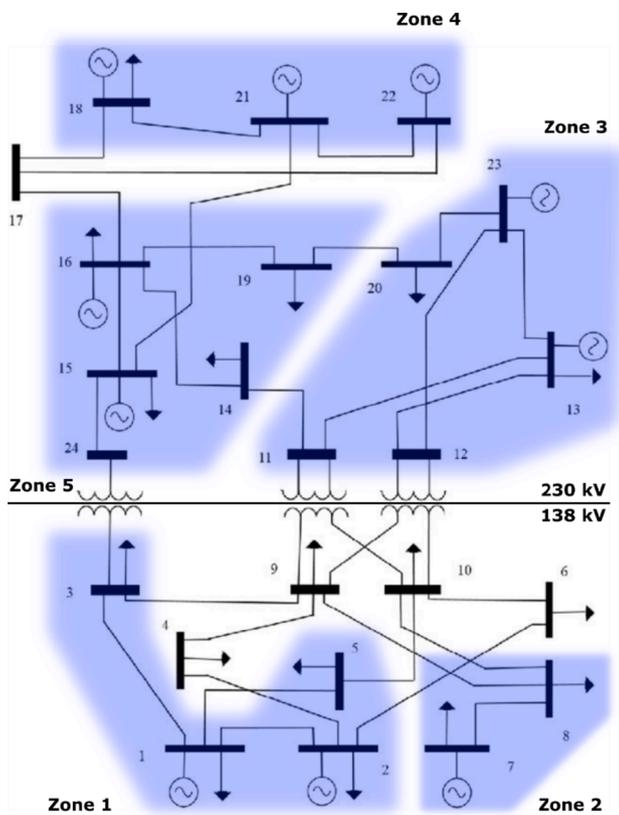

Fig. 6. Modified IEEE 24-bus test system showing the defined zones.

Table 2
Zones of the test system under analysis, and the corresponding buses and utilities within.

Zone	Buses	Utilities
Z1	1, 2, 3, 5	U1, U2, U3, U4
Z2	7, 8	U5
Z3	11, 12, 13, 20, 23	U6, U13, U14
Z4	18, 21, 22	U10, U11, U12
Z5	14, 15, 16, 19, 24	U7, U8, U9

costs represented as coefficients of a quadratic cost function model as described in [17]. In the decentralized operation paradigm, the utilities do not have knowledge of the full grid topology (incidence matrix is unknown), only having knowledge of transmission line connections inside their respective zones.

It can be observed that the designated zones are diverse in terms of both size and structure. This was intended to test the versatility of the proposed algorithm. Furthermore, load buses 4, 6, 9, and 10 are not incorporated in any zone and therefore historical information from them is only provided when the energy cloud / cooperative information exchange is enabled.

This way, they are considered as self-managing microgrids (with self-consumption) which can still share their activation vectors in the proposed scheme for every new system state, however, have no control actions over the system. In this sense, the case study can also demonstrate the applicability of the proposed algorithm for the decentralized management of interconnected multi-microgrids with varying sizes, local generation capacity, and self-consumption.

3.2. Synthetically generated historical data

To synthetically generate the historical dataset of centralized operation (as described in Section 2.1), that reflects realistic conditions, a typical transmission systems' annual load profile provided by the Portuguese Energy Regulation Services Entity (ERSE) was used. The load profile is high resolution (15-minute) for the full year of 2019 (35040 time steps).

To apply the normalized load profile to the current network, the annual peak load was set to correspond to the marginal operation of the network at maximum loadability (considering bus voltage angle and transmission line power limits). To determine this, the network is modeled and simulated using MATPOWER 7.0 [41], and the total load of the system is gradually increased by incrementing individual bus loads while maintaining their original power factor (pf).

The maximum loadability occurs at the point when any infinitesimal increase in individual bus loads would render an AC-OPF solution infeasible (violating network constraints). By performing this, the maximum loadability of this network was found to be 3334.50 MW (total load). The maximum (active power) loadability of individual load buses (PD^{max}) and their pf is detailed in Table 4 (note that non-load buses have a pf of zero).

In this way, the normalized typical load (based on Portuguese transmission systems) can be applied to the current network by setting the annual peak load at each bus to its maximum loadability. A synthesized historical dataset could now be generated by performing the

Table 3

Utilities of the test system under analysis (considered the decentralized operating agents) including the zone association, incorporated generator number, and the coefficients for the individual generator cost functions.[1]

Utility	Bus	Zone	Incorporated Generators	PG^{min}	PG^{max}	a	b	c	MUT	MDT	RD, RU	SU	SD	IH
U1	B1	Z1	G1, G2	16	20	400.7	130	0	1	1	30	5	5	−10
U2	B1	Z1	G3, G4	15.2	76	212.3	16.1	0.01414	8	4	20	596	596	10
U3	B2	Z1	G5, G6	16	20	400.7	130	0	1	1	30	5	5	−10
U4	B2	Z1	G7, G8	15.2	76	212.3	16.1	0.01414	8	4	20	596	596	10
U5	B7	Z2	G9, G10, G11	25	100	781.5	43.7	0.05267	8	8	70	566	250	6
U6	B13	Z3	G12, G13, G14	69	197	832.8	48.6	0.00717	12	10	30	775	443	−8
U7	B15	Z5	G16, G17, G18, G19, G20	2.4	12	86.4	56.6	0.32841	4	2	10	68	38	−3
U8	B15	Z5	G21	54.3	155	382.2	12.4	0.00834	8	8	30	953	260	12
U9	B16	Z5	G22	54.3	155	382.2	12.4	0.00834	8	8	30	953	260	12
U10	B18	Z4	G23	100	400	395.4	4.42	0.00021	1	1	200	0	0	20
U11	B21	Z4	G24	100	400	395.4	4.42	0.00021	1	1	200	0	0	20
U12	B22	Z4	G25, G26, G27, G28, G29, G30	10	50	0.001	0.001	0	0	0	50	0	0	8
U13	B23	Z3	G31, G32	54.3	155	382.2	12.4	0.00834	8	8	30	953	260	8
U14	B23	Z3	G33	140	350	665.1	11.9	0.0049	24	48	40	4468	1915	8

[1] Quadratic cost function coefficients are a, b, and c. PG^{min}, PG^{max}, MUT, MDT, RD, RU, SU, and SD are the min/max generation limits, min/max up/down times, ramp up/down costs, and start up/down costs, respectively.

Table 4

Maximum loadability (peak annual load) at each load bus and corresponding pf.

Load Bus	pf	PD^{max} (MW)	Load Bus	pf	PD^{max} (MW)	Load Bus	pf	PD^{max} (MW)
1	0.9799	126.36	**7**	0.9806	146.25	**15**	0.9802	370.89
2	0.9794	113.49	**8**	0.9797	200.07	**16**	0.9806	117.00
3	0.9795	210.60	**9**	0.9795	204.75	**18**	0.9798	389.61
4	0.9801	86.58	**10**	0.9796	228.15	**19**	0.9797	211.77
5	0.9811	83.07	**13**	0.9799	310.05	**20**	0.9800	149.76
6	0.9795	159.12	**14**	0.9804	226.98	**Peak Annual Load**		3334.50

following steps:

Step 1: Calculate active power load at each bus *b,* and the corresponding reactive power load, for each timestep in the load profiles.

$$PD_b^{hist,t} = P_t^{typical} \cdot PD_b^{max}, \quad \forall b \in \{1, 2, \cdots 24\}, t \in \{1, 2, \cdots, 35040\} \quad (22)$$

$$QD_b^{hist,t} = PD_b^{hist,t} \cdot pf_b, \quad \forall b \in \{1, 2, \cdots 24\}, t \in \{1, 2, \cdots, 35040\} \quad (23)$$

Step 2: Perform a deterministic AC-OPF calculation to determine the corresponding active power generation levels of each utility, for each timestep in the load profiles.

users with self-consumption by local generation, and therefore the considered load profiles for the transmission system already account for renewable generation and self-consumption on the distribution system level, according to Portuguese electrical systems design and operating conditions.

Second, the synthetically generated historical operation data does not consider events such as outages, line failures, unit maintenance, etc. While these events have an impact on power flow, the proposed method is a pure ML one. I.e., their presence in the historical data does not affect the algorithm and/or results since there is no physical model, only a statistical one.

Such events would simply be addition input variables in the NW-KDE

$$\{PG_{U1}^{hist,t}, PG_{U2}^{hist,t}, \cdots, PG_{U14}^{hist,t}\} \xleftarrow{AC-OPF} \begin{Bmatrix} PD_1^{hist,t}, PD_2^{hist,t}, \cdots, PD_{24}^{hist,t} \\ QD_1^{hist,t}, QD_2^{hist,t}, \cdots, QD_{24}^{hist,t} \end{Bmatrix}, \quad \forall t \in \{1, 2, \cdots, 35040\} \quad (24)$$

With this a historical dataset for a full year (15-minute resolution) is obtained. The day of the year and hour of the day are added as independent input variables in addition to the power loads at all buses. The total load for the generated historical operation is plotted in Fig. 7.

Two assumptions made to construct this case study are duly noted and justified. The first assumption is regarding the presence of renewable generation in the system. In a modern SG, renewable generation sources are indispensable and therefore must be incorporated. This is done by choosing the ERSE profiles which correspond to aggregated

activation function generator if the new case corresponds to the same situation. The scope of this paper is to propose, implement, and validate the proposed algorithm. For the purpose of having a benchmark study and a control experiment, such events are therefore not considered to ensure proper testing and validation of the implemented algorithm, but are recommended to be studied in future work.

Step 3: In accordance with the conceptual model presented in Section 2.1, decompose the historical dataset into local datasets available for each agent/utility in the system according to their local variables.
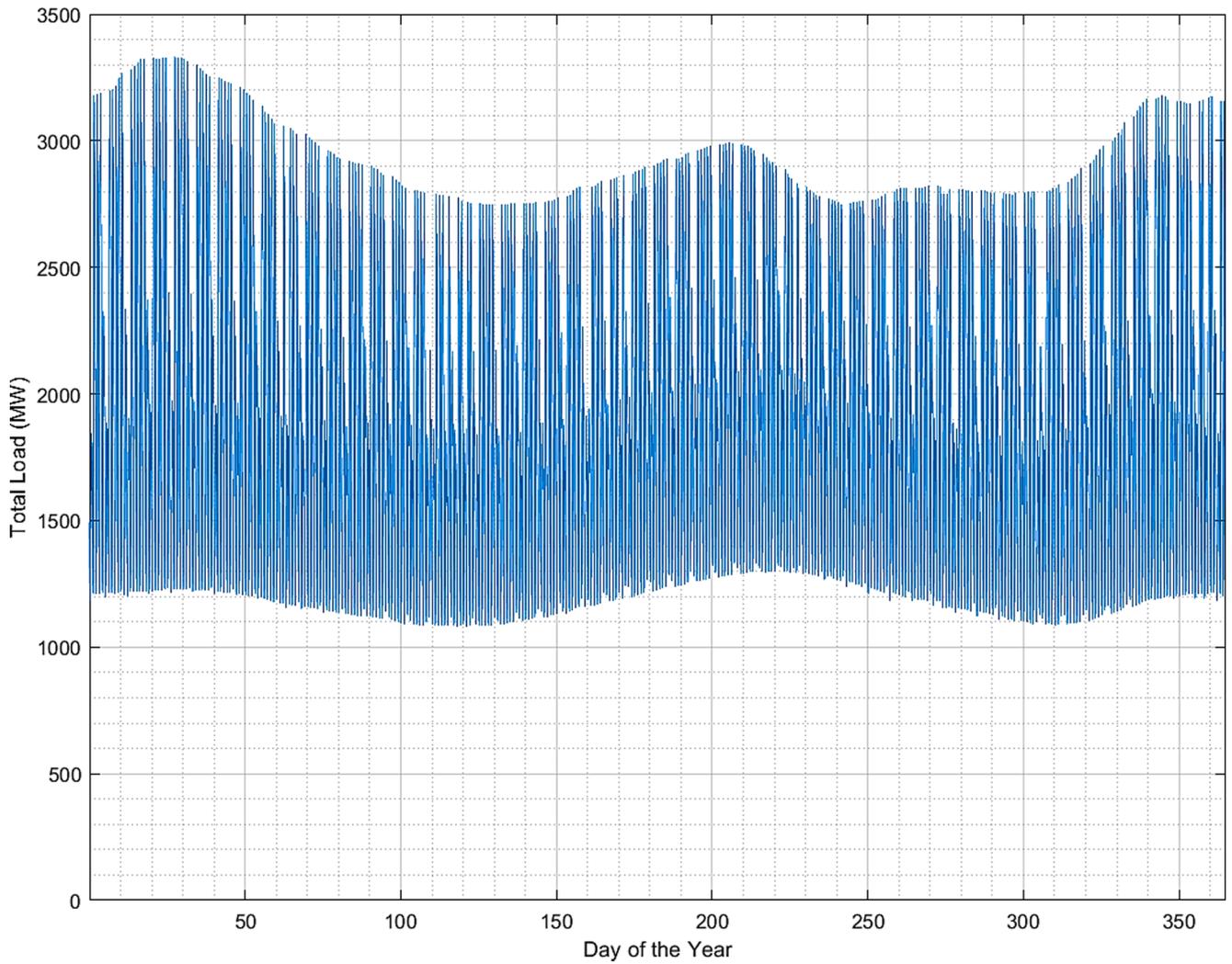
Fig. 7. Plot of the historical total load (1 year with 15-minute resolution.)

With the local datasets extracted, each agent can then employ the proposed methodology in Section 2.2. and participate in the cooperative information exchange cloud model described in Section 2.3.

To demonstrate the local datasets available to each agent U1 is taken as an example, which is located at bus 1 (B1) in zone 1 (Z1). By referring to Table 2, Z1 contains buses 1, 2, 3, and 5. Therefore, for U1, N_V is equal

to 6 (load values at four buses, hour of the day, day of the year). By applying this to all utilities, the local historical datasets are represented in (25)-(38), being the extension of (5) considering locally available information. With this, the proposed algorithm can now be implemented locally at each utility.

$$\textbf{\textit{at U}}1: \quad H_k = \left\{ \underbrace{PG_{U1}^{hist,t}}_{\text{historical generation U1}}, \underbrace{PD_1^{hist,t}, PD_2^{hist,t}, PD_3^{hist,t}, PD_5^{hist,t}}_{\text{historical load values in Zone 1 (U1)}}, \underbrace{\tau(t)}_{\text{hour of the day}}, \underbrace{\delta(t)}_{\text{day of the year}} \right\}, \quad \forall t \in \{1, 2, ..., 35040\} \tag{25}$$

$$\textbf{\textit{at U}}2: \quad H_k = \left\{ \underbrace{PG_{U2}^{hist,t}}_{\text{historical generation U2}}, \underbrace{PD_1^{hist,t}, PD_2^{hist,t}, PD_3^{hist,t}, PD_5^{hist,t}}_{\text{historical load values in Zone 1 (U2)}}, \underbrace{\tau(t)}_{\text{hour of the day}}, \underbrace{\delta(t)}_{\text{day of the year}} \right\}, \quad \forall t \in \{1, 2, ..., 35040\} \tag{26}$$

$$\textbf{\textit{at U}}3: \quad H_k = \left\{ \underbrace{PG_{U3}^{hist,t}}_{\text{historical generation U3}}, \underbrace{PD_1^{hist,t}, PD_2^{hist,t}, PD_3^{hist,t}, PD_5^{hist,t}}_{\text{historical load values in Zone 1 (U3)}}, \underbrace{\tau(t)}_{\text{hour of the day}}, \underbrace{\delta(t)}_{\text{day of the year}} \right\}, \quad \forall t \in \{1, 2, ..., 35040\} \tag{27}$$

$$\text{at } U4: \quad H_k = \left\{ \underbrace{PG_{U4}^{hist,t}}_{\text{historical generation } U4}, \underbrace{PD_1^{hist,t}, PD_2^{hist,t}, PD_3^{hist,t}, PD_5^{hist,t}}_{\text{historical load values in Zone 1 } (U4)}, \underbrace{\tau(t)}_{\text{hour of the day}}, \underbrace{\delta(t)}_{\text{day of the year}} \right\}, \quad \forall t \in \{1, 2, ..., 35040\} \tag{28}$$

$$\text{at } U5: \quad H_k = \left\{ \underbrace{PG_{U5}^{hist,t}}_{\text{historical generation of } U5}, \underbrace{PD_7^{hist,t}, PD_8^{hist,t}}_{\text{historical load values in Zone 2 } (U5)}, \underbrace{\tau(t)}_{\text{hour of the day}}, \underbrace{\delta(t)}_{\text{day of the year}} \right\}, \quad \forall t \in \{1, 2, ..., 35040\} \tag{29}$$

$$\text{at } U6: \quad H_k = \left\{ \underbrace{PG_{U6}^{hist,t}}_{\text{historical generation } U6}, \underbrace{PD_{11}^{hist,t}, PD_{12}^{hist,t}, PD_{13}^{hist,t}, PD_{20}^{hist,t}, PD_{23}^{hist,t}}_{\text{historical load values in Zone 3 } (U6)}, \underbrace{\tau(t)}_{\text{hour of the day}}, \underbrace{\delta(t)}_{\text{day of the year}} \right\}, \quad \forall t \in \{1, 2, ..., 35040\} \tag{30}$$

$$\text{at } U7: \quad H_k = \left\{ \underbrace{PG_{U7}^{hist,t}}_{\text{historical generation } U7}, \underbrace{PD_{14}^{hist,t}, PD_{15}^{hist,t}, PD_{16}^{hist,t}, PD_{19}^{hist,t}, PD_{24}^{hist,t}}_{\text{historical load values in Zone 5 } (U7)}, \underbrace{\tau(t)}_{\text{hour of the day}}, \underbrace{\delta(t)}_{\text{day of the year}} \right\}, \quad \forall t \in \{1, 2, ..., 35040\} \tag{31}$$

$$\text{at } U8: \quad H_k = \left\{ \underbrace{PG_{U8}^{hist,t}}_{\text{historical generation } U8}, \underbrace{PD_{14}^{hist,t}, PD_{15}^{hist,t}, PD_{16}^{hist,t}, PD_{19}^{hist,t}, PD_{24}^{hist,t}}_{\text{historical load values in Zone 5 } (U8)}, \underbrace{\tau(t)}_{\text{hour of the day}}, \underbrace{\delta(t)}_{\text{day of the year}} \right\}, \quad \forall t \in \{1, 2, ..., 35040\} \tag{32}$$

$$\text{at } U9: \quad H_k = \left\{ \underbrace{PG_{U9}^{hist,t}}_{\text{historical generation } U9}, \underbrace{PD_{14}^{hist,t}, PD_{15}^{hist,t}, PD_{16}^{hist,t}, PD_{19}^{hist,t}, PD_{24}^{hist,t}}_{\text{historical load values in Zone 5 } (U9)}, \underbrace{\tau(t)}_{\text{hour of the day}}, \underbrace{\delta(t)}_{\text{day of the year}} \right\}, \quad \forall t \in \{1, 2, ..., 35040\} \tag{33}$$

$$\text{at } U10: \quad H_k = \left\{ \underbrace{PG_{U10}^{hist,t}}_{\text{historical generation } U10}, \underbrace{PD_{18}^{hist,t}, PD_{21}^{hist,t}, PD_{22}^{hist,t}}_{\text{historical load values in Zone 4 } (U10)}, \underbrace{\tau(t)}_{\text{hour of the day}}, \underbrace{\delta(t)}_{\text{day of the year}} \right\}, \quad \forall t \in \{1, 2, ..., 35040\} \tag{34}$$

$$\text{at } U11: \quad H_k = \left\{ \underbrace{PG_{U11}^{hist,t}}_{\text{historical generation } U11}, \underbrace{PD_{18}^{hist,t}, PD_{21}^{hist,t}, PD_{22}^{hist,t}}_{\text{historical load values in Zone 4 } (U11)}, \underbrace{\tau(t)}_{\text{hour of the day}}, \underbrace{\delta(t)}_{\text{day of the year}} \right\}, \quad \forall t \in \{1, 2, ..., 35040\} \tag{35}$$

$$\text{at } U12: \quad H_k = \left\{ \underbrace{PG_{U12}^{hist,t}}_{\text{historical generation } U12}, \underbrace{PD_{18}^{hist,t}, PD_{21}^{hist,t}, PD_{22}^{hist,t}}_{\text{historical load values in Zone 4 } (U12)}, \underbrace{\tau(t)}_{\text{hour of the day}}, \underbrace{\delta(t)}_{\text{day of the year}} \right\}, \quad \forall t \in \{1, 2, ..., 35040\} \tag{36}$$

$$\text{at } U13: \quad H_k = \left\{ \underbrace{PG_{U13}^{hist,t}}_{\text{historical generation } U13}, \underbrace{PD_{11}^{hist,t}, PD_{12}^{hist,t}, PD_{13}^{hist,t}, PD_{20}^{hist,t}, PD_{23}^{hist,t}}_{\text{historical load values in Zone 3 } (U13)}, \underbrace{\tau(t)}_{\text{hour of the day}}, \underbrace{\delta(t)}_{\text{day of the year}} \right\}, \quad \forall t \in \{1, 2, ..., 35040\} \tag{37}$$

$$\text{at } U14: \quad H_k = \left\{ \underbrace{PG_{U14}^{hist,t}}_{\text{historical generation } U14}, \underbrace{PD_{11}^{hist,t}, PD_{12}^{hist,t}, PD_{13}^{hist,t}, PD_{20}^{hist,t}, PD_{23}^{hist,t}}_{\text{historical load values in Zone 3 } (U14)}, \underbrace{\tau(t)}_{\text{hour of the day}}, \underbrace{\delta(t)}_{\text{day of the year}} \right\}, \quad \forall t \in \{1, 2, ..., 35040\} \tag{38}$$

3.3. Performed analyses

The case study is now fully constructed, and validation studies can be performed. Using the generated historical datasets, the proposed algorithm is tested by employing a fully decentralized week-ahead operation planning for OPF in the grid with very high-resolution (15 min). The total system load profile for the test week, shown in Fig. 8, was generated based on the average summer values of the yearly load profile. Individual input variables (bus loads) at each time step are generated by maintaining the ratio of load buses in the test system and dividing the total system load accordingly. Three studies were performed:

Study 1: In the first study the validity of the proposed algorithm is demonstrated, and the influence of tunable parameters is showcased. In this study, the full algorithm is employed, including the cooperative information exchange scheme between the agents. Coefficients α_i were defined as follows:

- α_{in}: coefficient for historical input variables from sources which are physically connected to the utility (i.e. load values of the same bus).
- α_{out}: coefficient for historical input variables which are not physically connected to the utility (i.e. load value of bus other than that of the utility).
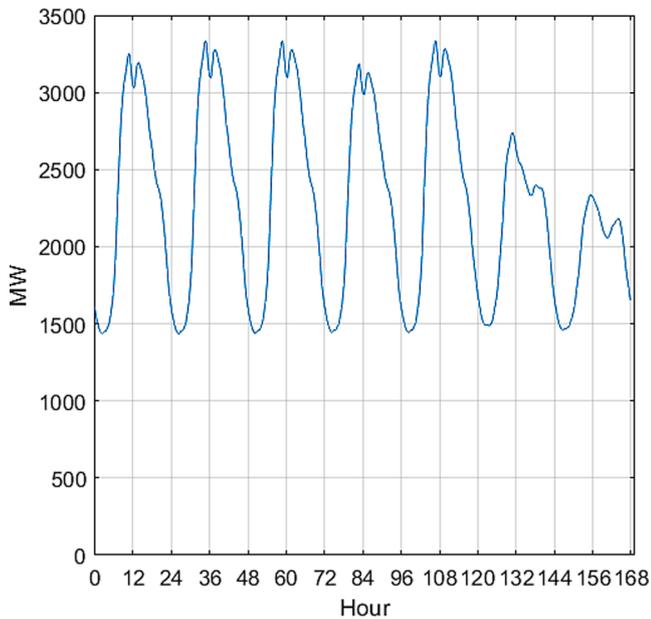
Fig. 8. Total load profile for the considered test week (15-minute resolution).

- $\alpha_{hour}, \alpha_{day}$: coefficients the day of the year and hour of the day for each historical case, respectively.

Study 2: In the second study, the proposed cloud-based cooperative information exchange is investigated by comparing the results for each agent with and without the exchanged activation functions.

Study 3: In the third and final case study, the performance of the proposed algorithm is assessed in comparison with a NN.

For all studies, the results are compared against the centralized scenario with a deterministic AC-OPF solution using MATPOWER. The results of all three studies are presented subsequently in the next section.

4. Simulation results

4.1. Study 1: Validation and parameter tuning

In the first study, the proposed algorithm is validated and the effect of tunable parameters (normalized bandwidth coefficients α_i and N_S) is assessed. Two scenarios are compared. In the first, all normalized bandwidth coefficients α_i are set to 0.5. This can be considered the "default" value of the coefficients. In the second scenario, the coefficients are tuned by generating random value combinations until the error falls below a certain threshold. Both scenarios are assessed relative to the exact values obtained by a centralized AC-OPF solution. Here, it is noted that on the machine used for implementation, the algorithm run time was recorded to be less than 4 s. Tuning the parameters ran in less than 1 min for each utility. This was around the same time that the training time of the NN used in the third study[3]. Therefore, the tuning process was very fast, even for the demanding high-resolution week-ahead test case considered.

Plots of the results of the ideal generation levels of all utilities controlled by each of the decentralized operating agents are shown in Fig. 9, and the detailed results for all utilities are listed in Table 5. It is noted that U1, U3, and U12 are found to have a zero-load factor throughout the test week as the act as baseload generators for the network. The load factor of each utility is shown in Fig. 10 based on the centralized OPF solution. Therefore the baseload generation utilities U1,

U3, and U12 were excluded from the results of this study and the two subsequent ones. The overloaded operating conditions that were used to assert the effectiveness of the proposed method can be seen in Fig. 10, with all generation centers being committed throughout the entire test week. By analyzing the obtained results shown in Fig. 9 and Table 5, several detailed observations can be.

First, with tuned parameters the moving average percentage error (MAPE), relative to that of the centralized AC-OPF solution, was well below 0.1% for all utilities in all zones. In all the plots of Fig. 10, it is seen that the lines corresponding to the exact centralized OPF solution and those of the predicted values using the proposed algorithm are tightly overlayed, being hardly distinguishable.

Second, using untuned parameters set to the default arbitrary values (10 for Ns and 0.5 for α_{out}, α_{in}, α_{day}, and α_{hour}), the ideal generation profile was still estimated using the proposed algorithm with very high accuracy. Apart from U6 in Zone 3, the ideal generation levels of all utilities in the network were accurately predicted with a MAPE less than or equal to 1%, which is very satisfactory for a worst-case performance without using any parameter tuning or information exchange.

Third, it is noted that the utilities predictions most affected by parameter tuning were U5 (Zone 2) and U6 (Zone 3), both of which incorporate large high-cost generators resulting in the high-frequency fluctuations during peak load hours. For those utilities parameter tuning, using the tuned parameters successfully resulted in dropping the MAPE to below 0.1%. U7 was similarly critical due to the three acute ramps in generation during the test week, which were also very accurately predicted after parameter tuning with a MAPE of less than 0.1%. Finally, U10 and U11 being high load factor utilities (Fig. 10) and in an energy exporting zone (Fig. 11) were sensitive to parameter tuning (although the untuned solution still had a 1% error, which is satisfactory for being the worst-case performance scenario).

By performing this study, the validity of the proposed algorithm was demonstrated, and the influence of tunable parameters was showcased. With proper parameter tuning, the algorithm was shown to be exceptionally accurate in predicting the ideal generation levels for each decentralized agent in the decentralized operation paradigm, relying solely on locally available historical data and with neither knowledge of the physical grid model, nor any raw information exchange between the zones. The robustness of the proposed algorithm was showcased by guaranteeing satisfactory prediction accuracy even when using untuned, arbitrarily chosen parameters, which serves as the worst-case operation scenario.

4.2. Study 2: Effect of cooperative information exchange

In the second study, the effect of the proposed cloud-based information exchange framework was investigated. In this case, two scenarios are simulated and compared: using tuned parameters but with and without the incorporated cooperative information exchange framework. Once again, the MAPE of predicted ideal generation levels of each utility is calculated he exact values of the centralized AC-OPF solution. The simulation results of this study are shown in Fig. 12 and Table 6. By analyzing these results, the following observations are made.

First, the results show that incorporating the proposed cloud-based cooperative information exchange framework results in a profound improvement in the accuracy of all predicted generation values. By using the activation code sharing method formulated in Section 2, all the decentralized agents in all zones were capable of reducing their ideal generation prediction errors to less than 0.1% without divulging any raw information or having any knowledge of the physical grid model.

Second, by referring to the data in Table 3 and the metrics in Fig. 11, one can see that the cooperative information exchange framework proves to be most beneficial for utilities that have expensive generators and exist in zones that are net exporters of energy. This is expected, since such utilities would heavily rely on any information from other parts of the grid since they mainly respond to peak loads or to zones that are net
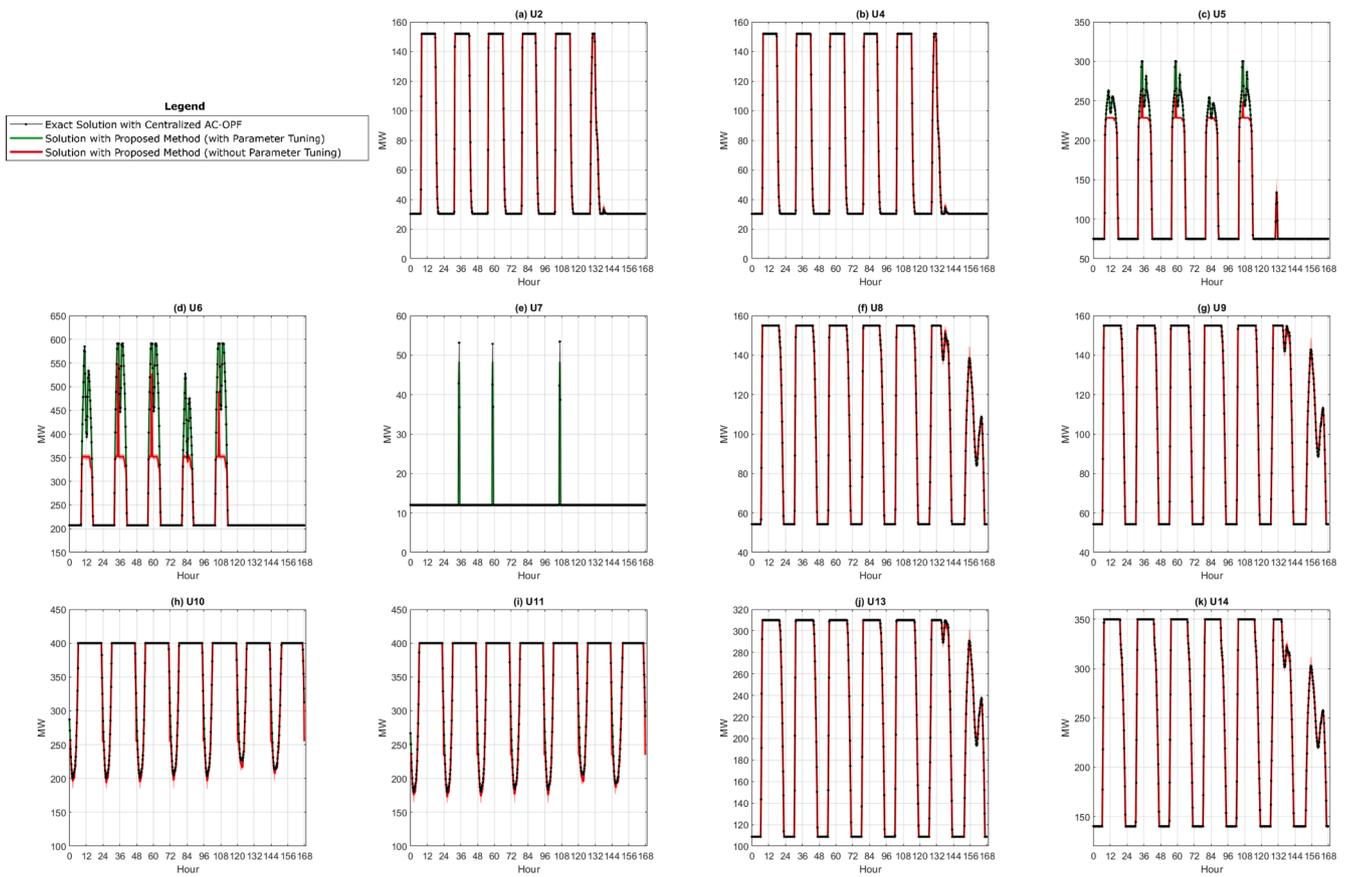
---

[3] Rrecorded run times were obtained as an average 1000 runs to account for variations.

Fig. 9. Results of the first study: predicted week-ahead generation profile (15-minute resolution) by each utility, with and without parameter tuning, compared with a centralized solution.

Table 5
Results of the first study: tuned parameters and MAPE.

Utility	Scenario	Tunable Parameters					MAPE
		N_S	α_{out}	α_{in}	α_{day}	α_{hour}	
U2 (Zone 1)	U2 - Default	10	0.50	0.50	0.50	0.50	0.3790 %
	U2 - Tuned	**9**	**0.05**	**0.60**	**0.90**	**0.70**	**0.0386 %**
U4 (Zone 1)	U4 - Default	10	0.50	0.50	0.50	0.50	0.3788 %
	U4 - Tuned	**9**	**0.05**	**0.95**	**0.70**	**0.95**	**0.0383 %**
U5 (Zone 2)	U5 - Default	10	0.50	0.50	0.50	0.50	2.2590 %
	U5 - Tuned	**16**	**0.05**	**0.55**	**0.90**	**0.40**	**0.0573 %**
U6 (Zone 3)	U6 - Default	10	0.50	0.50	0.50	0.50	6.1020 %
	U6 - Tuned	**25**	**0.05**	**0.45**	**0.75**	**0.80**	**0.0534 %**
U7 (Zone 5)	U7 - Default	10	0.50	0.50	0.50	0.50	0.9695 %
	U7 - Tuned	**4**	**0.05**	**0.30**	**0.85**	**0.35**	**0.0628 %**
U8 (Zone 5)	U8 - Default	10	0.50	0.50	0.50	0.50	0.3234 %
	U8 - Tuned	**36**	**0.05**	**0.40**	**0.95**	**0.55**	**0.0328 %**
U9 (Zone 5)	U9 - Default	10	0.50	0.50	0.50	0.50	0.3041 %
	U9 - Tuned	**9**	**0.05**	**0.35**	**0.75**	**0.65**	**0.0338 %**
U10 (Zone 4)	U10 - Default	10	0.50	0.50	0.50	0.50	0.9498 %
	U10 - Tuned	**36**	**0.05**	**1.00**	**0.70**	**0.40**	**0.0500 %**
U11 (Zone 4)	U11 - Default	10	0.50	0.50	0.50	0.50	1.0449 %
	U11 - Tuned	**25**	**0.05**	**0.10**	**0.95**	**0.55**	**0.0474 %**
U13 (Zone 3)	U13 - Default	10	0.50	0.50	0.50	0.50	0.3104 %
	U13 - Tuned	**25**	**0.05**	**1.00**	**0.55**	**0.95**	**0.0275 %**
U14 (Zone 3)	U14 - Default	10	0.50	0.50	0.50	0.50	0.2732 %
	U14 - Tuned	**25**	**0.05**	**0.15**	**0.80**	**1.00**	**0.0221 %**

importers of energy in the grid. This is most evident by through the results of U10 in Zone 4. Being in the top energy exporting region of the grid, using the proposed cooperative information exchange allows the U10 operator to completely diminish the decentralized prediction error from 8.07 % to 0.05%.

Finally, the influence of parameter tuning vs. the cooperative information exchange functionality can be compared by comparing the results of this study vs. the previous one. Overall, It can be seen that the impact of the implemented cooperative information sharing model is higher than parameter tuning, both in terms of the confidence intervals (evident by relative narrowing of the shaded regions of the plots in each of Fig. 9 and Fig. 12), and overall accuracy (MAPE). With this being said,
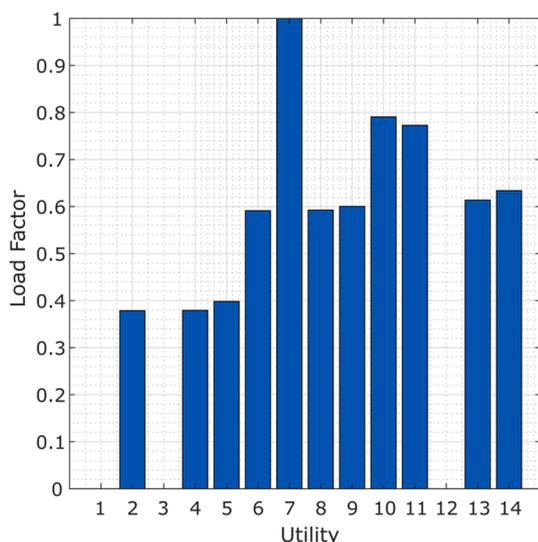
Fig. 10. Average load factors of the utilities.
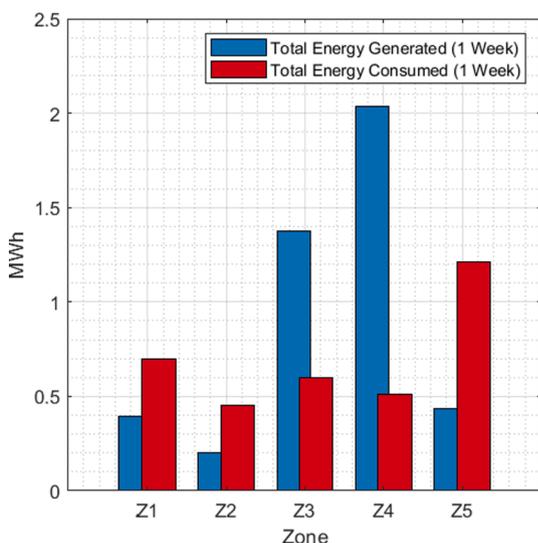
Fig. 11. Total energy import/export by each zone for the considered week.

it is seen that there are specific cases where either functionality contributes to the prediction accuracy more significantly than the other. In the case of U8, the proposed algorithm has a MAPE of 0.033 %. Removing the information exchange capability greatly increases the MAPE to 8.07 % (Table 6), while using untuned parameters causes a much smaller increase to 0.323 % (Table 5). U6 exhibits the opposite behavior, as using untuned parameters causes the MAPE to increase from 0.057 % to 6.10 % (Table 5), while removing the cooperative information exchange capability on results in a slight increase to 0.069 % (Table 6). This suggests that parameter tuning is critical for more large expensive generation centers with high-frequency fluctuations during peak hours such as U6, while participating in the cloud-based cooperative information exchange framework is more beneficial for expensive generators in zones that are net energy exporters in the network.

4.3. Study 3: Comparison with Neural network

In this third and final study a prediction of the ideal generation values of each utility is obtained using a NN, to serve as a comparison between the developed ML algorithm a well-establish one. The same local historical datasets used as the inputs for the proposed algorithm are

used to train the NN for each individual agent. In this case, the results of the proposed model and that of the NN, both being decentralized solutions, are evaluated by evaluating the MAPE based on the centralized AC-OPF. The NN was trained and simulated for the zone that exhibited the highest MAPE in its respective zone (with tuned parameters and cooperative information exchange): U2 from Z1, U5 from Z2, U6 from Z3, U10 from Z4, and U7 from Z5. By inspecting the results shown in Fig. 13 and Table 7, the following points are noted.

First, the proposed algorithm significantly outperforms the NN for all cases. The NN guarantees a MAPE less than 0.5% , while for the proposed method the MAPE is less than 0.1% for all cases. In terms of the computational speed, it was mentioned that the training time of the NN was around the same time as the tuning process of the proposed algorithm. However, a key difference is the fact that the NN training process must be rerun for any new output variable introduced, while the proposed algorithm is tuned once for each utility / agent.

With this being said, the proposed algorithm not only outperforms the NN in terms of accuracy but also in terms of computational time, since the proposed method's average running time is 4 s (for the high-resolution week-ahead test case considered). It is also important to note that the NN network results are dependent on the training process which contains random elements, i.e., the results of the NN are different each time the training process is re-run (hence the averaged results presented in Table 7). This is not the case for the proposed algorithm, which provides the same results given the same historical dataset being used, being more reliable than a NN. The results of the first case study it was shown that the proposed algorithm provides accurate predictions even without parameter tuning, guaranteeing a much more robust applicability compared to a conventional NN algorithm.

Finally, it is very important to note is that one of the main novel contributions of the proposed algorithm is its capability to accommodate cooperative information exchange to enhance the results of individual agents. A NN implementation (and other ML algorithms) does not accommodate this, since local datasets are used to train the NN. Therefore, to improve the NN results it would be required to further augment or pre-process the historical data itself, and afterwards reperform the training process. In the case of the proposed algorithm, the designed cooperative information exchange framework allows agents to improve their results dynamically while the algorithm is running, adding a significant level of versatility to the proposed approach as opposed to a NN and other ML algorithms (not to mention the higher computational efficiency).

5. Discussion and recommendations for future work

The proposed framework and algorithm open the door for various applications such as decentralized operation of multi-microgrid networks and active distribution system management considering the uncertainty of renewable power generation. The proposed cooperative information exchange also provides opportunities for transactive information exchange using peer-to-peer or cloud-based platforms for cooperative operation by decentralized agents. This main objective of this paper was to present the developed algorithm and validate its applicability using the case studies as a novel ML algorithm. To pave the way for real-life applicability of this framework, follow-up studies should be performed to investigate the performance of the algorithm further. With this paper being the first to present the newly developed algorithm, several paths for future work building on it are identified subsequently.

The main requirement to deploy the proposed algorithm is to ensure the compliance of the infrastructure needed to deploy this algorithm for real-world SGs: I.e., communication infrastructure, market conditions, in addition to the legal and regulatory prerequisites for the decentralized operation paradigm. For real-world SGs and decentralized operating agents to fully benefit from all the advantages of this algorithm, these conditions must be met, and the infrastructure must be operational.
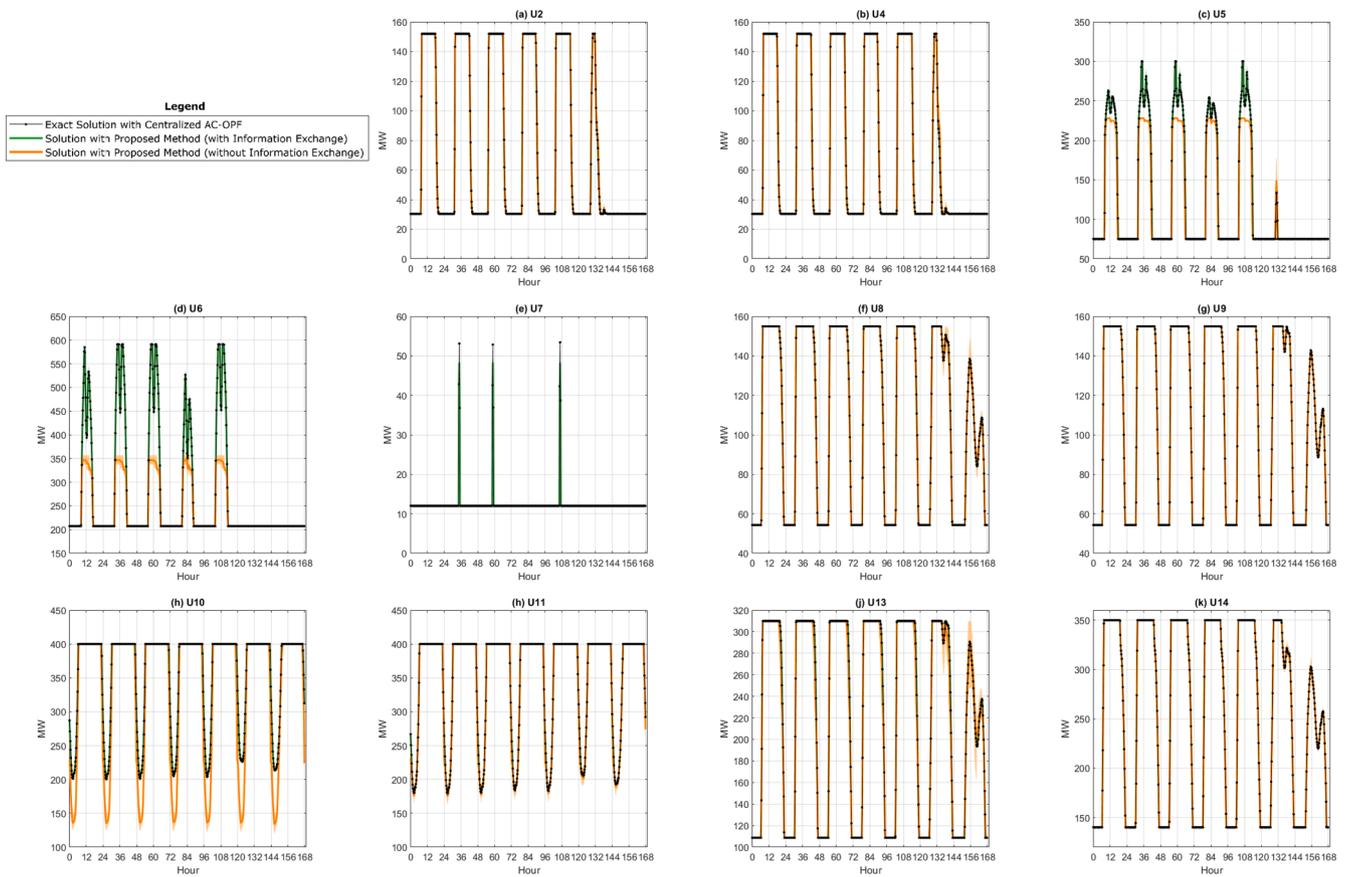
Fig. 12. Results of the second study: predicted week-ahead generation profile (15-minute resolution) by each utility, with and without information exchange, compared with a centralized solution.

Table 6
Results of the second study: MAPE for each utility with and without the implemented cooperative information exchange.

Utility	Scenario	MAPE
U2 (Zone 1)	**With Proposed Cooperative Information Exchange**	**0.0386 %**
	Without Information Exchange	0.6760 %
U4 (Zone 1)	**With Proposed Cooperative Information Exchange**	**0.0383 %**
	Without Information Exchange	0.9969 %
U5 (Zone 2)	**With Proposed Cooperative Information Exchange**	**0.0573 %**
	Without Information Exchange	3.6187 %
U6 (Zone 3)	**With Proposed Cooperative Information Exchange**	**0.0534 %**
	Without Information Exchange	0.0694 %
U7 (Zone 5)	**With Proposed Cooperative Information Exchange**	**0.0628 %**
	Without Information Exchange	0.9695 %
U8 (Zone 5)	**With Proposed Cooperative Information Exchange**	**0.0328 %**
	Without Information Exchange	0.4277 %
U9 (Zone 5)	**With Proposed Cooperative Information Exchange**	**0.0338 %**
	Without Information Exchange	0.0321 %
U10 (Zone 4)	**With Proposed Cooperative Information Exchange**	**0.0500 %**
	Without Information Exchange	8.0720 %
U11 (Zone 4)	**With Proposed Cooperative Information Exchange**	**0.0474 %**
	Without Information Exchange	0.7267 %
U13 (Zone 3)	**With Proposed Cooperative Information Exchange**	**0.0275 %**
	Without Information Exchange	1.1598 %
U14 (Zone 3)	**With Proposed Cooperative Information Exchange**	**0.0221 %**
	Without Information Exchange	0.2732 %

While this is the global direction, there is still some follow-up work that must be performed to investigate the requirements needed by the communication infrastructure (i.e. cloud-based communication), decentralized grids (structure of systems such as multi-microgrids), and the nature of transactive information being a newly introduced concept in this work.

It is important to note that the aforementioned points do not preclude in any way from the fact that the proposed algorithm is fully deployable for modern-day SGs with infrastructures already in place. In the worst-case scenario, the full benefits of the algorithm will not be retained, and the performance will still be better than widely available ML algorithms as was demonstrated. However, there will be a loss of the potential improvement brought about by the cooperative information sharing capability. In realistic terms, operators will not be inclined to invest in deploying a new method unless they are sure its benefits are worth the effort. Thus, follow-up work must be performed 1) to concretely demonstrate this from an algorithm analysis perspective, and 2) from the point of view of overlapping research fields (i.e., informatics, economics, and legislature) to fully pave the way for the transition to this new paradigm.

From an algorithm analysis perspective, several future studies are recommended. First, a full sensitivity analysis of the physical grid considered is recommended, which would compare the algorithm performance when applied to power grids of different sizes, topologies, and densities (number of lines vs. number of buses). Second, the effect of the level of decentralization (which corresponds to the resulting number of decentralized agents or operating zones) on the performance of the algorithm should be evaluated. In the context of decentralized operation, the existence of multiple zones exists *a priori*. With the zones of operation corresponding to different decentralized operating agents, the physical definition of the zones is what the method is applied and adapted to, rather than being an imposition by the method itself. In real applications the zones can range from different individual prosumers in an energy community, to different micro-grid operators in a multi-microgrid system. The application of the proposed method to similar newly proposed physical models of decentralized power systems should be investigated, and interactions such as the effect of merging of several
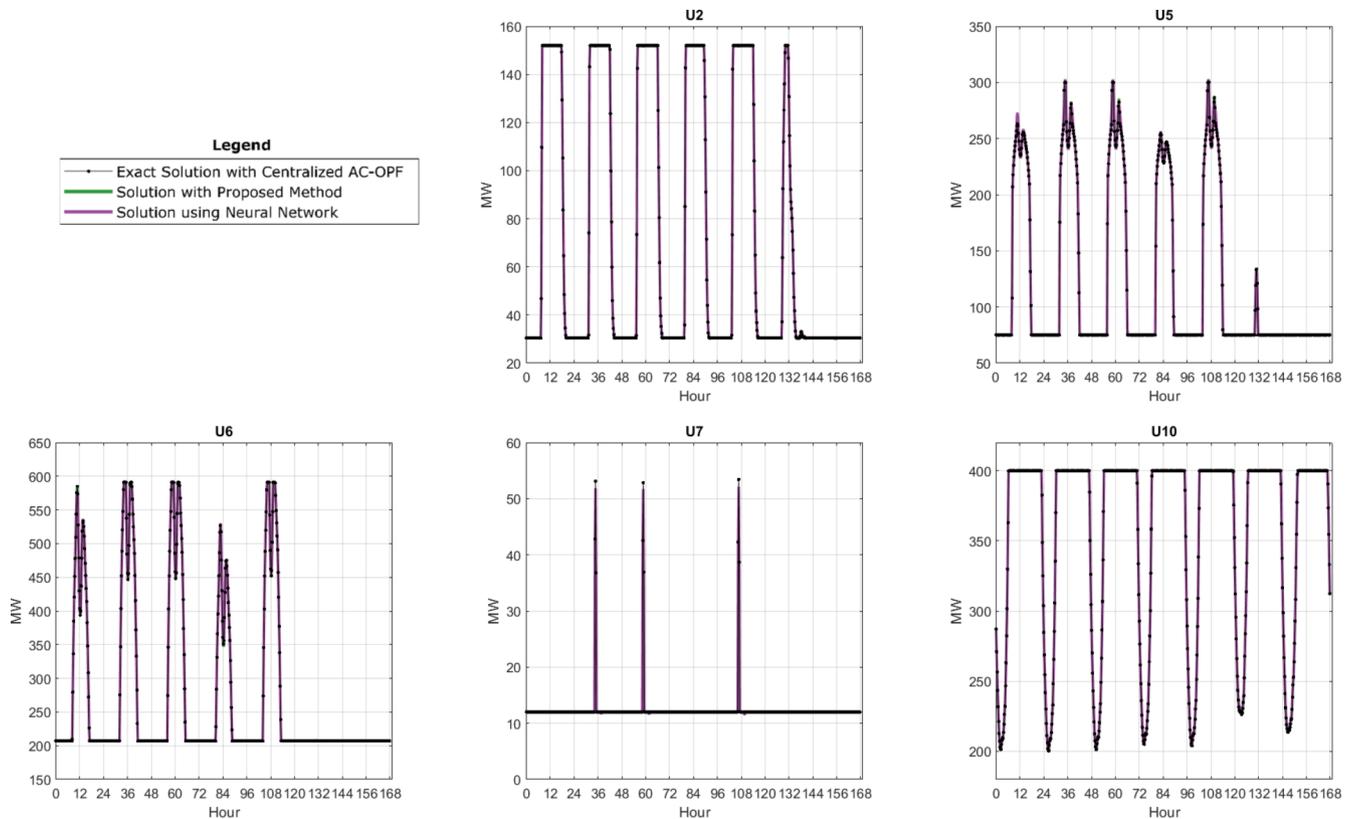
peer or cloud-based platforms for cooperative operation by decentralized agents.

Authors Contributions

M. Lotfi, C. Monteiro, G.J. Osório, and M.S. Javadi worked on the conceptualization and methodology. M. Lotfi and C. Monteiro worked on the implementation of the proposed approach and computational simulations. M. Lotfi worked on the manuscript writing and data visualization. M.S. El Moursi and J.P.S. Catalão worked on the validation of the results, manuscript revision, and supervision. All the authors have read, reviewed, and agree to the submitted version of the manuscript.

Declaration of Competing Interest

The authors declare that they have no known competing financial interests or personal relationships that could have appeared to influence the work reported in this paper.

References

[1] Abbasi AR. Probabilistic Load Flow Based on Holomorphic Embedding, Kernel Density Estimator and Saddle Point Approximation Including Correlated Uncertainty Variables. Electr Power Syst Res 2020;183:106178. https://doi.org/10.1016/j.epsr.2019.106178.

[2] Abdi H, Beigvand SD, Scala ML. A review of optimal power flow studies applied to smart grids and microgrids. Renew Sustain Energy Rev 2017;71:742–66.

[3] Alimi, O. A., Ouahada, K., & Abu-Mahfouz, A. M. (2020). A Review of Machine Learning Approaches to Power System Security and Stability. In *IEEE Access* (Vol. 8, pp. 113512–113531). Institute of Electrical and Electronics Engineers Inc. https://doi.org/10.1109/ACCESS.2020.3003568.

[4] Allan RN, Da Silva Am, Burchett RC. Evaluation methods and accuracy in probabilistic load flow solutions. IEEE Transactions on Power Apparatus and Systems 1981;PAS-100(5):2539–46. https://doi.org/10.1109/TPAS.1981.316721.

[5] Beltrán JC, Aristizábal AJ, López A, Castaneda M, Zapata S, Ivanova Y. Comparative analysis of deterministic and probabilistic methods for the integration of distributed generation in power systems. *Energy Rep, September*. 2020;6:88–104. https://doi.org/10.1016/j.egyr.2019.10.025.

[6] Borkowska B. Probabilistic Load Flow. IEEE Trans Power Apparatus Systems 1974; PAS-93(3):752–9. https://doi.org/10.1109/TPAS.1974.293973.

[7] Cao J, Yan Z. Probabilistic optimal power flow considering dependences of wind speed among wind farms by pair-copula method. Int J Electr Power Energy Syst 2017;84:296–307. https://doi.org/10.1016/j.ijepes.2016.06.008.

[8] Capitanescu F. Critical review of recent advances and further developments needed in AC optimal power flow. Electr Power Syst Res 2016;136:57–68. https://doi.org/10.1016/j.epsr.2016.02.008.

[9] Christakou K, Tomozei DC, Le Boudec JY, Paolone M. AC OPF in radial distribution networks – Part I: On the limits of the branch flow convexification and the alternating direction method of multipliers. Electr Power Syst Res 2017;143: 438–50. https://doi.org/10.1016/j.epsr.2016.07.030.

[10] Christakou K, Tomozei DC, Le Boudec JY, Paolone M. AC OPF in radial distribution networks – Part II: An augmented Lagrangian-based OPF algorithm, distributable via primal decomposition. Electr Power Syst Res 2017;150:24–35. https://doi.org/10.1016/j.epsr.2017.04.028.

[11] Constante-Flores GE, Illindala MS. Data-driven probabilistic power flow analysis for a distribution system with renewable energy sources using Monte Carlo simulation. IEEE Trans Ind Appl 2019;55(1):174–81. https://doi.org/10.1109/TIA.2018.2867332.

[12] Cruz M, Fitiwi D, Santos S, Mariano S, Catalao JPS. Multi Flexibility Options Integration to Cope with Large-Scale Integration of Renewables. IEEE Trans Sustainable Energy 2018;3029(c):1–12. https://doi.org/10.1109/TSTE.2018.2883515.

[13] Ergun H, Dave J, Van Hertem D, Geth F. Optimal Power Flow for AC-DC Grids: Formulation, Convex Relaxation, Linear Approximation, and Implementation. IEEE Trans Power Syst 2019;34(4):2980–90. https://doi.org/10.1109/TPWRS.2019.2897835.

[14] Espinosa-Juárez E, Hernández A. A method for voltage sag state estimation in power systems. IEEE Trans Power Delivery 2007;22(4):2517–26. https://doi.org/10.1109/TPWRD.2007.905587.

[15] Green J, Newman P. Citizen utilities: The emerging power paradigm. Energy Policy 2017;105:283–93. https://doi.org/10.1016/j.enpol.2017.02.004.

[16] Hatziargyriou ND, Karakatsanis TS, Papadopoulos M. Probabilistic load flow in distribution systems containing dispersed wind power generation. Probabilistic Load Flow In Distribution Systems Containing Dispersed Wind Power Generation. 1993;8(1):159–65.

[17] Javadi MS, Firuzi K, Rezanejad H, Lotfi M, Gough M, Catalão JPS. Optimal Sizing and Siting of Electrical Energy Storage Devices for Smart Grids Considering Time-of-Use Programs. IECON 2019–45th Annual Conference of the IEEE Industrial Electronics Society 2019.

[18] Kamalov F. Kernel density estimation based sampling for imbalanced class distribution. Inf Sci 2020;512:1192–201. https://doi.org/10.1016/j.ins.2019.10.017.

[19] Kotsalos K, Miranda I, Silva N, Leite H. A horizon optimization control framework for the coordinated operation of multiple distributed energy resources in low voltage distribution networks. Energies 2019;12(6):1182. https://doi.org/10.3390/en12061182.

[20] Lin W, Yang Z, Yu J, Bao S, Dai W. Toward fast calculation of probabilistic optimal power flow. IEEE Trans Power Syst 2019;34(4):3286–8. https://doi.org/10.1109/TPWRS.2019.2911050.

[21] Liu Y, Gao S, Cui H, Yu L. Probabilistic load flow considering correlations of input variables following arbitrary distributions. Electr Power Syst Res 2016;140: 354–62. https://doi.org/10.1016/j.epsr.2016.06.005.

[22] Lotfi M, Javadi M, Osório GJ, Monteiro C, Catalão JPS. A novel ensemble algorithm for solar power forecasting based on kernel density estimation. Energies 2020;13 (1):216. https://doi.org/10.3390/en13010216.

[23] Lotfi M, Monteiro C, Shafie-Khah M, Catalao JPS. Evolution of Demand Response: A Historical Analysis of Legislation and Research Trends. 2018 20th International Middle East Power Systems Conference 2018. https://doi.org/10.1109/MEPCON.2018.8635264.

[24] Martirano L, Rotondo S, Kermani M, Massarella F, Gravina R. Power Sharing Model for Energy Communities of Buildings. IEEE Trans Ind Appl 2021;57(1):170–8. https://doi.org/10.1109/TIA.2020.3036015.

[25] Monteiro C, Ramirez-Rosado IJ, Fernandez-Jimenez LA, Ribeiro M. New probabilistic price forecasting models: Application to the Iberian electricity market. Int J Electr Power Energy Syst 2018;103:483–96. https://doi.org/10.1016/j.ijepes.2018.06.005.

[26] Morales JM, Pérez-Ruiz J. Point estimate schemes to solve the probabilistic power flow. IEEE Trans Power Syst 2007;22(4):1594–601. https://doi.org/10.1109/TPWRS.2007.907515.

[27] Munsing E, Mather J, Moura S. Blockchains for decentralized optimization of energy resources in microgrid networks. IEEE Conference on Control Technology and Applications (CCTA) 2017;2017:2164–71. https://doi.org/10.1109/CCTA.2017.8062773.

[28] Nosratabadi H, Mohammadi M, Kargarian A. Nonparametric Probabilistic Unbalanced Power Flow with Adaptive Kernel Density Estimator. IEEE Trans Smart Grid 2019;10(3):3292–300. https://doi.org/10.1109/TSG.2018.2823058.

[29] Pasetti M, Rinaldi S, Manerba D. A Virtual Power Plant Architecture for the Demand-Side Management of Smart Prosumers. Applied Sciences 2018;8(3):432. https://doi.org/10.3390/app8030432.

[30] Ren Z, Wang K, Li W, Jin L, Dai Y. Probabilistic Power Flow Analysis of Power Systems Incorporating Tidal Current Generation. IEEE Trans Sustainable Energy 2017;8(3):1195–203. https://doi.org/10.1109/TSTE.2017.2669139.

[31] Rosenblueth E. Point estimates for probability moments. Proc. Nat. Acad. Sci. 1975;72(10):3812–4.

[32] Schellenberg A, Rosehart W, Aguado J. Cumulant-based probabilistic optimal power flow (P-OPF) with Gaussian and Gamma distributions. IEEE Trans Power Syst 2005;20(2):773–81. https://doi.org/10.1109/TPWRS.2005.846184.

[33] Sedhom BE, El-Saadawi MM, El Moursi MS, Hassan MA, Eladl AA. IoT-based optimal demand side management and control scheme for smart microgrid. Int J Electr Power Energy Syst 2021;127:106674. https://doi.org/10.1016/j.ijepes.2020.106674.

[34] Su CL. Probabilistic load-flow computation using point estimate method. IEEE Trans Power Syst 2005;20(4):1843–51. https://doi.org/10.1109/TPWRS.2005.857921.

[35] Thirugnanam K, Moursi MSE, Khadkikar V, Zeineldin HH, Al Hosani M. Energy Management of Grid Interconnected Multi-Microgrids Based on P2P Energy Exchange: A Data Driven Approach. IEEE Trans Power Syst 2021;36(2):1546–62. https://doi.org/10.1109/TPWRS.2020.3025113.

[36] Viviani G, Heydt G. Stochastic Optimal Energy Dispatch. IEEE Transactions on Power Apparatus and Systems 1981;PAS-100(7):3221–8. https://doi.org/10.1109/TPAS.1981.316651.

[37] Wu C, Gu W, Zhou S, Chen X. Coordinated Optimal Power Flow for Integrated Active Distribution Network and Virtual Power Plants Using Decentralized Algorithm. IEEE Trans Power Syst 2021;36(4):3541–51. https://doi.org/10.1109/TPWRS.2021.3049418.

[38] Wu C, Jiang P, Sun Y, Zhang C, Gu W. Economic dispatch with CHP and wind power using probabilistic sequence theory and hybrid heuristic algorithm. J Renewable Sustainable Energy 2017;9(1):013303. https://doi.org/10.1063/1.4976144.

[39] Yang Z, Zhong H, Bose A, Zheng T, Xia Q, Kang C. A Linearized OPF Model with Reactive Power and Voltage Magnitude: A Pathway to Improve the MW-Only DC OPF. IEEE Trans Power Syst 2018;33(2):1734–45. https://doi.org/10.1109/TPWRS.2017.2718551.

[40] Zhang P, Lee ST. Probabilistic Load Flow Computation Using the Method of Combined Cumulants and Gram-Charlier Expansion. IEEE Trans Power Syst 2004;19(1):676–82. https://doi.org/10.1109/TPWRS.2003.818743.

[41] Zimmerman RD, Murillo-Sanchez CE, Thomas RJ. MATPOWER: Steady-State Operations, Planning and Analysis Tools for Power Systems Research and Education. IEEE Trans Power Syst 2011;26(1):12–9. https://doi.org/10.1109/TPWRS.2010.2051168.